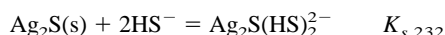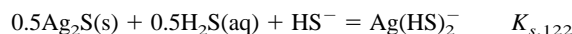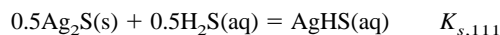**Pergamon**

Experimental determination of the stability and stoichiometry of sulphide complexes of silver(I) in hydrothermal solutions to 400°C

A. STEFÁNSSON* and T. M. SEWARD

Institut für Mineralogie und Petrographie, Eidgenössische Technische Hochschule, ETH-Zentrum, Sonneggstrasse 5,
CH-8092 Zürich, Switzerland

Abstract—The solubility of silver sulphide (acanthite/argentite) has been measured in aqueous sulphide solutions between 25 and 400°C at saturated water vapour pressure and 500 bar to determine the stability and stoichiometry of sulphide complexes of silver(I) in hydrothermal solutions. The experiments were carried out in a flow-through autoclave, connected to a high-performance liquid chromatographic pump, titanium sampling loop, and a back-pressure regulator on line. Samples for silver determination were collected via the titanium sampling loop at experimental temperatures and pressures. The solubilities, measured as total dissolved silver, were in the range 1.0×10^{-7} to 1.30×10^{-4} mol kg^{-1} (0.01 to 14.0 ppm), in solutions of total reduced sulphur between 0.007 and 0.176 mol kg^{-1} and pH$_{T,p}$ of 3.7 to 12.7. A nonlinear least squares treatment of the data demonstrates that the solubility of silver sulphide in aqueous sulphide solutions of acidic to alkaline pH is accurately described by the reactions

$$0.5Ag_2S(s) + 0.5H_2S(aq) = AgHS(aq) \qquad K_{s,111}$$

$$0.5Ag_2S(s) + 0.5H_2S(aq) + HS^- = Ag(HS)_2^- \qquad K_{s,122}$$

$$Ag_2S(s) + 2HS^- = Ag_2S(HS)_2^{2-} \qquad K_{s,232}$$

where AgHS(aq) is the dominant species in acidic solutions, $Ag(HS)_2^-$ under neutral pH conditions and $Ag_2S(HS)_2^{2-}$ in alkaline solutions. With increasing temperature the stability field of $Ag(HS)_2^-$ increases and shifts to more alkaline pH in accordance with the change in the first ionisation constant of H_2S(aq). Consequently, $Ag_2S(HS)_2^{2-}$ is not an important species above 200°C. The solubility constant for the first reaction is independent of temperature to 300°C, with values in the range $\log K_{s,111} = -5.79$ (± 0.07) to -5.59 (± 0.09), and decreases to -5.92 (± 0.16) at 400°C. The solubility constant for the second reaction increases almost linearly with inverse temperature from $\log K_{s,122} = -3.97$ (± 0.04) at 25°C to -1.89 (± 0.03) at 400°C. The solubility constant for the third reaction increases with temperature from $\log K_{s,232} = -4.78$ (± 0.04) at 25°C to -4.57 (± 0.18) at 200°C. All solubility constants were found to be independent of pressure within experimental uncertainties. The interaction between Ag$^+$ and HS$^-$ at 25°C and 1 bar to form AgHS(aq) has appreciable covalent character, as reflected in the exothermic enthalpy and small entropy of formation. With increasing temperature, the stepwise formation reactions become progressively more endothermic and are accompanied by large positive entropies, indicating greater electrostatic interaction. The aqueous speciation of silver is very sensitive to fluid composition and temperature. Below 100°C silver(I) sulphide complexes predominate in reduced sulphide solutions, whereas Ag$^+$ and AgClOH$^-$ are the dominant species in oxidised waters. In high-temperature hydrothermal solutions of seawater salinity, chloride complexes of silver(I) are most important, whereas in dilute hydrothermal fluids of meteoric origin typically found in active geothermal systems, sulphide complexes predominate. Adiabatic boiling of dilute and saline geothermal waters leads to precipitation of silver sulphide and removal of silver from solution. Conductive cooling has insignificant effects on silver mobility in dilute fluids, whereas it leads to quantitative loss of silver for geothermal fluids of seawater salinity. *Copyright © 2003 Elsevier Science Ltd*

1. INTRODUCTION

Data on the stability and stoichiometry of metal complexes are essential for the study of dissolution, transport, and depositional mechanisms of metals by hydrothermal fluids in the Earth's crust. Such data can be coupled to analytical data on natural fluid composition, obtained by analysis of fluid inclusions or hydrothermal fluids collected from active geothermal systems, to define the metal speciation and to gain an understanding of the processes controlling the chemistry of the

metals in natural hydrothermal fluids. Furthermore, thermodynamic data on metal complexes can be used to model the effects of boiling, cooling, and mixing on the metal transport. Unfortunately, many metal-ligand reactions of geochemical importance suffer from the lack of reliable, experimentally determined thermodynamic data to be able to carry out many of these simple calculations.

Unlike many metals, high-temperature experimentally obtained data exist for aqueous silver(I) complexes, including chloride complexes (e.g., Seward, 1976; Zotov et al., 1986; Gammons and Williams-Jones, 1995), hydroxide complexes (Kozlov et al., 1983), hydroxychlorido complexes (Zotov et al., 1982), and carbonate and hydroxycarbonate complexes

* Author to whom correspondence should be addressed at present address: Science Institute, University of Iceland, Dunhagi 3, 107 Reykjavík, Iceland (andri@erdw.ethz.ch).

(Kozlov, 1985). Sulphide complexes of silver(I) have also been studied. Treadwell and Hepenstick (1949) measured the solubility of acanthite at 20°C to pH of 7. Their results indicated that the solubility is pH independent under acidic conditions, whereas it increases dramatically at neutral pH. Treadwell and Hepenstick (1949) suggested that AgHS(aq) predominates under acidic conditions but were unable to interpret the results at neutral pH because of oxidation of H_2S in the experiments. Schwarzenbach et al. (1958) and Schwarzenbach and Widmer (1966) measured the solubility of freshly precipitated silver sulphide at 25 and 20°C and proposed the AgHS(aq), $Ag(HS)_2^-$, and $Ag_2S(HS)_2^{2-}$ complex stoichiometries in acidic, neutral, and alkaline aqueous sulphide solutions, respectively, and determined the solubility constants for the respective complexes. Melent'yev et al. (1969) measured the solubility of silver sulphide between 100 and 180°C using a radioactive trace technique. However, no attempt was made to determine the dominant complex stoichiometry or derive solubility constants. More recently, Wood et al. (1987) measured the solubility of the assemblage pyrite + pyrrhotite + magnetite + sphalerite + galena + argentite + gold + stibnite + bismuthinite + molybdenite between 200 and 350°C in aqueous acidic solutions containing up to 5.0 mol kg^{-1} NaCl. They were unable to estimate the complex stoichiometry and stability because of the narrow pH range and total sulphur concentrations investigated. The studies of Sugaki et al. (1987) and Gammons and Barnes (1989) are the most extensive ones at present on silver(I) sulphide complexes at high temperatures. Sugaki et al. (1987) measured the solubility of silver sulphide between 25 and 250°C in aqueous sulphide solutions with pH ranging from 3.7 to 10.6 and total sulphur between 0.3 and 4.1 mol kg^{-1}. However, their data carry quite large inherent analytical uncertainties. They interpreted their results in terms of dinuclear complexes with $Ag_2S(H_2S)(aq)$, $Ag_2S(H_2S)HS^-$, $Ag_2S(H_2S)(HS)_2^{2-}$, and $Ag_2S(HS)_2^{2-}$ stoichiometries. Gammons and Barnes (1989) determined the solubility of silver sulphide at 25 to 300°C and pH and total reduced sulphur between 5.8 and 7.3 and 0.2 and 1.4 m, respectively. They concluded that under these conditions, $Ag(HS)_2^-$ is the dominant complex stoichiometry and estimated the solubility of silver sulphide with respect to this complex.

The aim of the present study was to determine the stability and stoichiometry of silver(I) sulphide complexes in hydrothermal solutions over a wide range of pH conditions and temperature. This was done by measuring the solubility of crystalline silver sulphide (acanthite/argentite) in the system H_2O-H_2S-NaOH. For this purpose, a flow-through autoclave system was designed and constructed, which allowed for sampling of the experimental solution at temperature and pressure.

2. EXPERIMENTAL METHODS

The solubility measurements were carried out in a flow-through system (Fig. 1). The low-pressure part of the system was made of Pyrex glass, PEEK tubing and Teflon®. All the wetted, high-pressure parts were made of titanium. The experiments were performed in an autoclave (RMI, 0.2% Pd titanium alloy) with an internal diameter of 6.5 mm and a length of 200 mm and filled with grains of silver sulphide. Before use, the titanium tubes and the autoclave were baked overnight at 400°C in air, then rinsed with 65% HNO_3 and 37% HCl (Merck Suprapur®), followed by several washes with deionised water. In this way, a relatively inert, corrosion-resistant titanium oxide layer was

produced. A Varian high-performance liquid chromatographic (HPLC) pump supplied the inlet solution to the line, and the pressure was regulated by a Coretest back-pressure regulator (BPR). The flow rate of the solution was maintained constant, typically at 1 ml min^{-1} but could be varied from 0.01 to 10 ml min^{-1}.

The autoclave and a large part of the inlet titanium tube were placed in a large volume Carbolite oven, which controlled the temperature to within ±0.5°C. The temperature was also monitored by three thermocouples at the inlet and the outlet of the autoclave. These measured temperatures never differed by more than ±1°C from the stated temperature and were usually within ±0.5°C of each other. The pressure was measured using a titanium pressure sensor in the pressure module of the HPLC pump as well as with a pressure gauge connected to the rear end of the BPR. The two readings were never found to deviate from the set pressure by >5 bar.

Two different types of silver sulphide were used separately for the solubility experiments. Firstly, fine-grained silver sulphide solids (99.9%) available from Aldrich® were used. This material was recrystallised in situ at 300°C for 7 d in aqueous solutions of 0.3 mol kg^{-1} total sulphide and pH of ~7. Second, silver sulphide was synthesised by bubbling grade 2.0 H_2S gas through deoxygenated 0.3 mol kg^{-1} $AgNO_3$ solution for several minutes. The fine-grained black precipitate was washed with deionised water, dried under vacuum in the dark, and hydrothermally recrystallised in a manner similar to the former case. The material obtained in both cases had a dark grey metallic colour, and X-ray diffraction analysis confirmed it to be >90% argentite (high-temperature cubic form of $Ag_2S(s)$ with <10% of acanthite (low-temperature monoclinic form of $Ag_2S(s)$). No elemental silver or sulphur was detected.

The solutions used in the experiments were prepared from triple-distilled water and 50% NaOH solution available from Aldrich. To exclude oxygen, the water was boiled under vacuum in an ultrasonic bath, and then oxygen-free Ar gas was bubbled through the solution. This procedure was repeated several times. The deoxygenated Ar was produced by passing grade 4.8 Ar through a 50 cm long silica glass column filled with copper metal filings and maintained at 440°C. The reduced sulphur was added to the deoxygenated solution by passing an H_2S-Ar gas mixture through it at 20°C and 1.2 ± 0.2 bar. The gas mixtures were prepared using an Environics computer interfaced gas mixer from pure H_2S (grade 2.0) and deoxygenated Ar (grade 4.8).

The precipitation kinetics of silver sulphide from the experimental solutions were observed to be rapid upon cooling, especially in solutions of neutral pH. This was evident from black precipitates building up at the low-pressure end of the back pressure regulator (BPR) and clogging of the titanium capillary tube in the cooling jacket. Therefore, a special titanium loop in line was designed and used for sampling at high temperatures (≥100°C). The sampling loop allowed for sampling at the experimental temperature and pressure, thus preventing loss of silver from solution upon cooling and sampling. The sample loop configuration is shown schematically in Figure 1. Firstly, the flow-though system, including the sampling loop, was flushed at the experimental flow rate with fresh solution. Second, the flow was stopped and the sampling loop closed off from the line using two high-temperature SITEC titanium three-way valves. Third, the sampling loop was opened carefully using the three-way valve for liquid withdrawal while it was still closed to the line and the liquid taken into acid washed Pyrex glass beakers. All remaining solution was flushed out with N_2 gas. For every run, 2 to 10 samples of ~5 ml volume were collected. The samples for silver analyses were weighed, and 0.5 ml of 25% NH_3 (Merck Suprapur®) were added to the sample followed by 0.5 to 1.0 mL of 30% H_2O_2 (Merck Suprapur®) to oxidise the H_2S to SO_4. The samples were then acidified to 10% HNO_3 (Merck Suprapur®). The dilution factor was determined by weighing. The resulting solutions were analysed by a flame atomic absorption spectrometry using a Varian 840A spectrometer. Standard solutions were matrix matched to the samples. The precision of the analysis was found to be ±2% at the 95% confidence level. The accuracy of the sample preparation and analysis determined by treating samples of known silver concentration in the same way as for unknown experimental samples was ±5% and ±8% above and below 1.0×10^{-6} mol kg^{-1} silver, respectively. The detection limits of the silver analysis were found to be 1.0×10^{-7} mol kg^{-1} (0.01 ppm).

Liquid samples for determination of reduced sulphur and total sodium concentrations were collected directly from the inlet solution
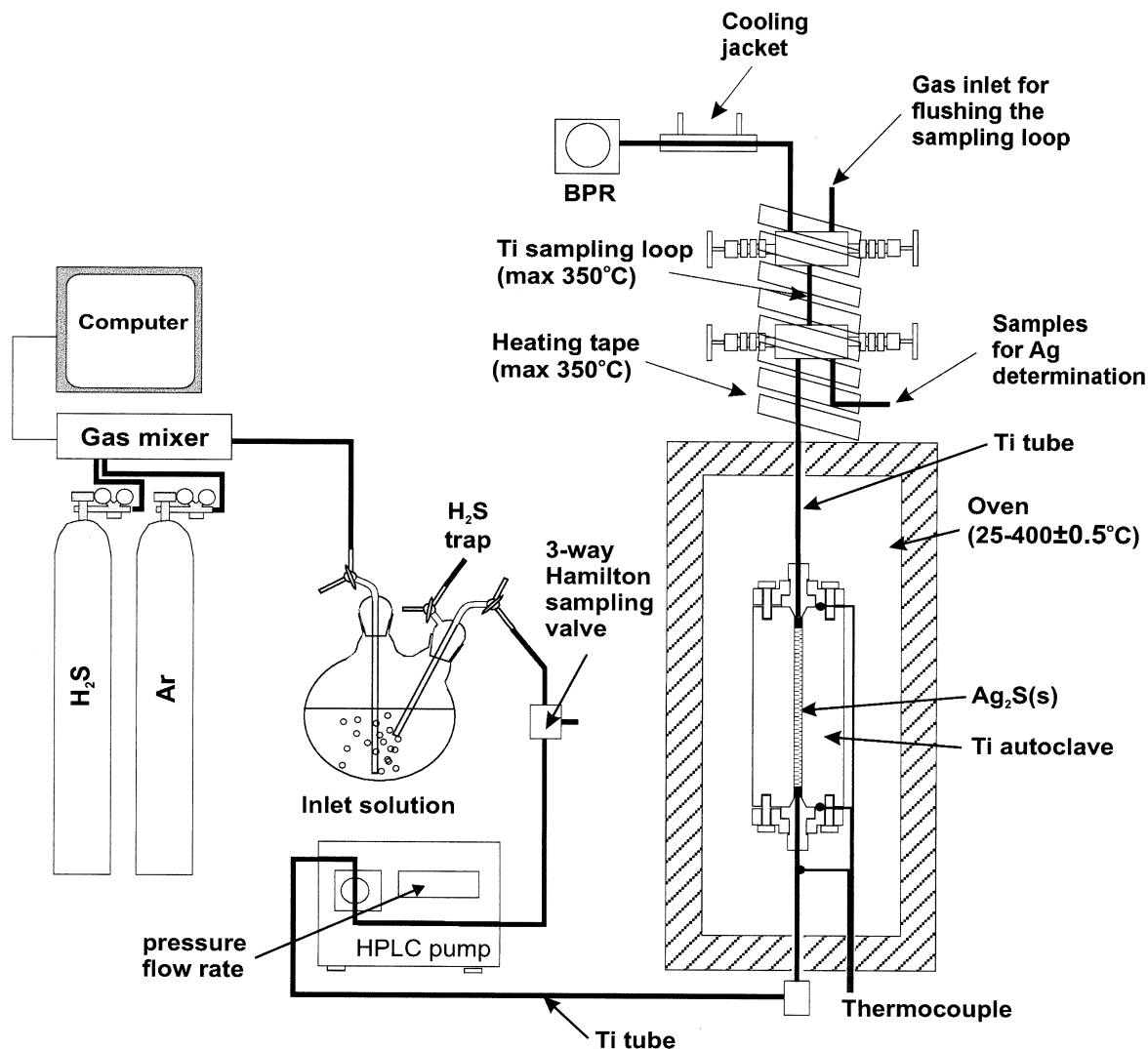
Fig. 1. Schematic picture of the experimental setup used in the present study. BPR = back-pressure regulator, HPLC = high-performance liquid chromatographic.

flask via a gas-tight Hamilton valve into polypropylene syringes. Total reduced sulphur was measured by iodometric back titration by adding 2 to 10 ml of solution to a flask containing a standardised 0.10 M iodine solution in an acetate buffer solution (pH ~ 4). The excess iodine was back titrated using a standardised 0.10-M $Na_2S_2O_3$ solution with starch as an indicator. The precision of the analyses was found to be ±3% at the 95% confidence level. Total sodium was determined by flame atomic emission spectrometry. The precision of the analyses was found to be ±3% at the 95% confidence level.

Additional static experiments were carried out at 25±0.5°C. Well-crystallised silver(I) sulphide was placed in a silica glass flask, the outer walls of which had been previously painted with black enamel to exclude light. The flask was flushed with oxygen-free Ar following addition of oxygen-free sulphide solution. Two Teflon® stopcocks and a gas-tight Hamilton sampling device were attached to the flask. This allowed samples to be withdrawn without air contamination. The samples were taken into gas-tight Hamilton syringe through a 0.2 μm Teflon® filter mounted into a polypropylene filter holder. The samples were treated in similar manner as for the flow-though experiments. The experimental duration ranged from 2 to 3 weeks to ensure equilibrium.

3. RESULTS

Total dissolved silver concentrations in equilibrium with silver sulphide were measured as a function of pH and total reduced sulphur between 25 and 350°C and at pressures corresponding to 10 to 30 bar above the saturated water vapour pressure as well as at 500 bar at temperatures from 100 to 400°C. The results are given in Appendix A and represent the results from 118 experimental runs. For each run, up to 10 samples were taken for the determination of dissolved silver concentration as well as 2 to 3 for the determination of total sulphur and sodium. The solubilities (i.e., total dissolved silver) were in the range from 1.0×10^{-7} to 1.30×10^{-4} mol kg^{-1} (0.01 to 14.0 ppm) in solutions of total reduced sulphur between 0.007 and 0.176 mol kg^{-1} and sodium between 0.00 and 0.41 mol kg^{-1}.

Considerable care was taken to establish that the solubilities measured represent equilibrium conditions. This was done in
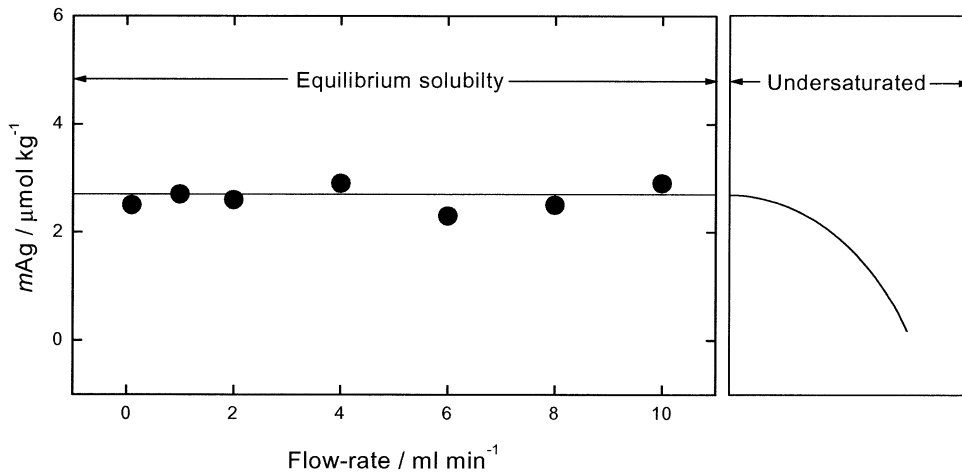
Fig. 2. Solubility of silver sulphide as a function of flow rate at 25°C and 1 bar in solution containing $mS_{total} = 0.131$ mol kg^{-1} and $mNaOH = 0.053$ mol kg^{-1}. The concentration plateau observed is considered to indicate equilibrium solubility.

two ways. First, the concentrations of the critical variables (mS_{total} and $mNaOH$) in the inlet solution were varied over a considerable range to obtain the stoichiometry and the respective equilibrium constants for the dominant aqueous silver complexes in solution. Second, following Mountain and Seward (1999), a concentration plateau at variable flow rate is considered to indicate equilibrium solubility. Several experiments were carried out to study the effect of flow rate on silver sulphide solubility. An example at 25°C and 1 bar, $mS_{total} = 0.131$ mol kg^{-1} and $mNaOH = 0.053$ mol kg^{-1}, is shown in Figure 2. As indicated, a concentration plateau is observed at all flow rates. However, all equilibrium solubility runs were carried out at 1 ml min^{-1}. At flow rates >10 ml min^{-1}, the solubility will eventually decrease when the residence times of the solutions in the silver sulphide column are less than the time needed to obtain equilibrium. The short equilibration time for silver sulphide is in good agreement with previous studies (Melent'yev et al., 1969; Gammons and Barnes, 1989), and similar observations have been made for copper sulphide solubility (Mountain and Seward, 1999).

4. COMPLEX FORMATION AND STABILITY CONSTANTS

4.1. Aqueous Speciation

The dissolution of silver sulphide in aqueous sulphide solution forming silver(I) sulphide complexes can be expressed by the general reaction of the form

$$\frac{x}{2} Ag_2S(s) + \left(y - \frac{x}{2}\right)HS^- + \left(\frac{x}{2} + z - y\right)H^+ = Ag_xS_yH_z^{x+z-2y}$$

(1)
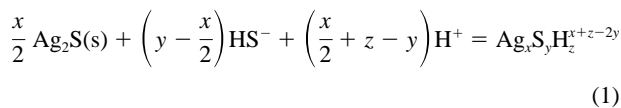
and the subsequent solubility constant is

$$K_{s,xyz} = m_{Ag_xS_yH_z^{x+z-2y}}\gamma_{Ag_xS_yH_z^{x+z-2y}}m_{H^+}^{y-z-x/2}\gamma_{H^+}^{y-z-x/2}m_{HS^-}^{x/2-y}\gamma_{HS^-}^{x/2-y}$$

(2)

In aqueous chloride free sulphide solution, silver(I) may be present as the free Ag$^+$ ion, hydroxide complexes and sulphide

complexes. Kozlov et al. (1983) concluded that silver(I) hydrolysed in aqueous alkaline solutions to form AgOH(aq) and Ag(OH)$_2^-$. Consequently, the total dissolved silver in aqueous sulphide solutions is defined as

$$mAg_{total} = \sum_x \sum_y \sum_z xm_{Ag_xS_yH_z^{x+z-y}} + m_{Ag^+} + m_{AgOH(aq)}$$

$$+ m_{Ag(OH)_2^-}$$ (3)

The solubility constants for silver sulphide with respect to Ag$^+$, AgOH(aq), and Ag(OH)$_2^-$ were estimated in this study from the thermodynamic properties of the aqueous species and the minerals. The results are given in Appendix B. The Gibbs free energy of H$_2$S(aq) was calculated from the experimentally determined Henry's law constant of H$_2$S (Suleimenov and Krupp, 1994) and the thermodynamic properties of H$_2$S(g) (Robie et al., 1979). The Gibbs free energy of Ag$^+$ was calculated from the AgCl(s) solubility measurements of Seward (1976) and the Gibbs free energy of aqueous Cl$^-$ (Cox et al., 1989) and AgCl(s) (Robie et al., 1979). The Gibbs free energy of aqueous AgOH(aq) and Ag(OH)$_2^-$ was estimated from the solubility data of Ag$_2$O(s) of Kozlov et al. (1983). The Gibbs free energy of Ag$_2$S(s), H$_2$O, and OH$^-$ were calculated from data given by Robie et al. (1979), Hill (1990), and Marshall and Franck (1981).

The solubility of silver sulphide was measured in the system H$_2$O-H$_2$S-NaOH, and the following species were considered in the data treatment: H$^+$, OH$^-$, H$_2$S(aq), HS$^-$, NaHS(aq), NaOH(aq), and Na$^+$, in addition to a given speciation model for silver(I) complexes defined by Eqn. [1] to [3]. The following independent reactions can be written for these aqueous species:

$$H_2O = H^+ + OH^-$$ (4)

$$NaOH(aq) = Na^+ + OH^-$$ (5)

$$H_2S(aq) = H^+ + HS^-$$ (6)

$$NaHS(aq) = Na^+ + HS^- \quad (7)$$
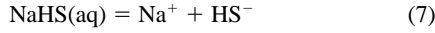
For these equilibrium reactions, the following equilibrium constants can be written:

$$K_w = m_{H^+}\gamma_{H^+}m_{OH^-}\gamma_{OH^-}a_{H_2O} \quad (8)$$

$$K_{NaOH} = m_{Na^+}\gamma_{Na^+}m_{OH^-}\gamma_{OH^-}m_{NaOH(aq)}^{-1}\gamma_{NaOH(aq)}^{-1} \quad (9)$$

$$K_{H_2S} = m_{H^+}\gamma_{H^+}m_{HS^-}\gamma_{HS^-}m_{H_2S(aq)}^{-1}\gamma_{H_2S(aq)}^{-1} \quad (10)$$

$$K_{NaHS} = m_{Na^+}\gamma_{Na^+}m_{HS^-}\gamma_{HS^-}m_{NaHS(aq)}^{-1}\gamma_{NaHS(aq)}^{-1} \quad (11)$$

The solution equilibria are also constrained by the charge balance

$$m_{H^+} + m_{Na^+} + m_{Ag^+} - m_{OH^-} - m_{HS^-} - m_{Ag(OH)_2^-}$$
$$+ \sum_x \sum_y \sum_z (x + z - y)m_{Ag_xS_yH_z^{x+z-y}} = 0 \quad (12)$$

and mass balances

$$mNa_{total} = m_{Na^+} + m_{NaOH(aq)} + m_{NaHS(aq)} \quad (13)$$

$$mS_{total} = m_{H_2S(aq)} + m_{HS^-} + m_{NaHS(aq)} + \sum_x \sum_y \sum_z ym_{Ag_xS_yH_z^{x+z-y}} \quad (14)$$

as well as the mass balance equation for aqueous silver defined by Eqn. [3] and the proton mass balance.

Most of the experimental solutions were dilute ($I = 4.4\times10^{-6}$ to 0.28 mol kg^{-1}). Therefore, the activity of water was taken to be unity as well as the activity coefficients for neutral aqueous species. Individual ion activity coefficients were estimated using a modified Debye-Hückel equation (Robinson and Stokes, 1968) of the form

$$\log\gamma_i = \frac{Az_i^2\sqrt{I}}{1 + \mathring{a}B\sqrt{I}} + \Gamma_\gamma + b_\gamma I \quad (15)$$

where A and B are Debye-Hückel parameters, taken to be equal to those for pure water; z is the ionic charge; $\mathring{a}$ is the ion size parameter, taken to be 9, 4, 3.5, 3.5, and 4 Å for H$^+$, Na$^+$, OH$^-$, HS$^-$, and silver complexes, respectively (Kielland, 1937); Γ_γ is a mole fraction to molality conversation factor; b_γ is an empirical correction factor (Helgeson et al., 1981); and I is the ionic strength, defined as

$$I = 0.5 \sum_i z_i^2 m_i \quad (16)$$

The aqueous speciation calculations and the determination of the solubility constants for silver sulphide were done simultaneously at a given temperature and pressure with the aid of the FITEQL computer program (Westall, 1982a, 1982b). For the present study, a subroutine was added to the program for calculation of ionic strength and individual ion activity coefficients. The calculation procedure to obtain the aqueous species activities and the solubility constants for silver sulphide was as follows: (1) The aqueous speciation was obtained by solving the equilibrium reactions (Eqn. 2 and 8 to 11) and the mass balance equations (Eqn. 3, 13, and 14) for a given silver(I) speciation model in an iterative manner using a Newton-Raph-

son algorithm. The equilibrium constants used for the calculations are given in Appendix B. In addition, an initial guess for the unknown silver(I) sulphide solubility constant was introduced. (2) Using these aqueous molalities, the solution ionic strength and the corresponding individual activity coefficients were calculated, and a new estimate for the silver sulphide solubility constants was made using a nonlinear least square procedure. (3) These new solubility constants were then used to recalculate the aqueous speciation from which new values of ionic strength, individual ion activity coefficients, and new estimates for the solubility constants for silver sulphide were calculated. Further repetitions of the procedure were continued until changes in the ionic strength and silver sulphide solubility constants were negligible.

Different silver(I) speciation models were fitted to the data. The goodness of the fit of a given model to the experimental data was quantified with the overall variance, V, normalised for number of degrees of freedom:

$$V = \frac{\sum \left(\dfrac{m_{Ag}^m - m_{Ag}^c}{s}\right)^2}{n_p n_{II} - n_u} \quad (17)$$

where m_{Ag}^m and m_{Ag}^c are the measured and modeled silver concentrations, n_p is the total number of data points, n_{II} is the number of components for which both total and free concentrations are known, and n_u is the number of silver(I) species in the model.

The dominant aqueous sodium and sulphide species in all the solutions were calculated to be Na$^+$ and H$_2$S(aq) and HS$^-$ with mNa^+/mNa_{total} in the range 84 to 100% and generally $>$99% and with $(mH_2S(aq)+mHS^-)/mS_{total}$ in the range 91 to 100% and generally $>$98%. The ion pairs NaHS(aq) and NaOH(aq) were never found to be significant and usually accounted for $<$1% of total S and Na, respectively. Therefore, both NaOH(aq) and NaHS(aq) could have been ignored in the speciation calculations without influencing the calculated silver sulphide solubility constants. The total measured aqueous silver concentration was always found to be orders of magnitude below the total sulphide concentrations, with mAg/mS_{total} ratios between 0.0002 and 0.11%. Therefore, the complexation of silver with sulphide had no significant influence on the aqueous sulphide speciation.

One of the largest uncertainties in calculating aqueous species activities and the silver sulphide solubility constants is the estimation of individual activity coefficients. The approach used in the present study was to minimise these problems by working at low ionic strength. The calculated ionic strength was in the range $I = 4.4\times10^{-6}$ to 0.28 mol kg^{-1} and was generally $<$0.05 mol kg^{-1}. Therefore, in all cases except for the few runs at high ionic strength ($0.10 > I > 0.28$ mol kg^{-1}), the activity coefficients are determined by the Debye-Hückel equation (i.e., accounting for long-range ion-ion interaction), and the term $b_\gamma I$ in Eqn. [15] is thus negligible. Furthermore, at low ionic strength, the activity of water and neutral aqueous species are effectively unity.

The calculations of the critical species activities, aH^+, aH_2S, and aHS^-, for the determination of the silver sulphide solubility constants are therefore solely based on that the total sulphide and sodium hydroxide concentrations, the first ionisation

Table 1. Nonlinear least squares fits for selected speciation models to the data at 25°C and 1 bar; the model given in bold type (i.e., model 6) was considered to best fit the data.
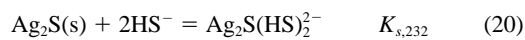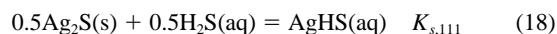
Model no.	Species	$\log K_s$	V
1	AgHS(aq)	−5.52	9.8
2	$Ag(HS)_2^-$	−3.66	13.8
3	$Ag(HS)_3^{2-}$	−2.84	20.2
4	$Ag_2S(HS)_2^{2-}$	4.67	19.0
5	AgHS(aq)	−5.63	
	$Ag(HS)_2^-$	−3.85	5.77
6	**AgHS(aq)**	**−5.62**	**0.352**
	$\mathbf{Ag(HS)_2^-}$	**−3.97**	
	$\mathbf{Ag_2S(HS)_2^{2-}}$	**−4.78**	
7	$HAg(HS)_2(aq)$	−4.54	2.61
	$Ag(HS)_2^-$	−3.92	
	$Ag_2S(HS)_2^{2-}$	−4.75	
8	$Ag_2(HS)_2(aq)$	−5.34	1.23
	$Ag(HS)_2^-$	−3.94	
	$Ag_2S(HS)_2^{2-}$	−4.75	
9	AgHS(aq)	−5.53	3.28
	AgS^-	−18.47	
	$Ag_2S(HS)_2^{2-}$	−4.70	
10	AgHS(aq)	−5.63	2.17
	$Ag_2S(H_2S)HS^-$	−3.86	
	$Ag_2S(HS)_2^{2-}$	−4.73	
11	AgHS(aq)	−5.61	24.8
	$Ag(HS)_2^-$	−3.94	
	$Ag(HS)_3^{2-}$	−3.57	
12	Ag^+	No convergence	
	AgHS(aq)		
	$Ag(HS)_2^-$		
	$Ag_2S(HS)_2^{2-}$		
13	Ag_2HS^+	No convergence	
	AgHS(aq)		
	$Ag(HS)_2^-$		
	$Ag_2S(HS)_2^{2-}$		

constant of H_2S(aq) and the ionisation constant of water, all of which are accurately known at the experimental conditions. The measured molalities of sulphide and sodium hydroxide (as mNaOH) based on replicate analysis were ±3% at the 95% confidence level, and the ionisation constant of water is accurately known over wide ranges of temperatures and pressures (Marshall and Franck, 1981). The first ionisation of constant of H_2S(aq) has recently been accurately determined to 350°C at saturated water vapour pressure in our laboratory (Suleimenov

and Seward, 1997). For the experiments at 500 bar, the first ionisation constant of H_2S was corrected for pressure using the volume of reaction reported by Ellis and McFadden (1972). The cumulative uncertainties on the calculated aqueous activities of critical species were generally within ±0.03 on the log scale to 350°C and somewhat higher at 400°C. Therefore, the primary errors in the calculated silver sulphide solubility constants are the uncertainties on the measured aqueous silver concentration.

4.2. Complex Stoichiometry and Silver Sulphide Solubility

Several speciation models were fitted to the data at each temperature. An example of the results of the fits and the speciation models applied at 25°C is given in Table 1. As indicated, the fit assuming AgHS(aq), $Ag(HS)_2^-$, and $Ag_2S(HS)_2^{2-}$ gave the lowest overall variance, V (Eqn. 17). The contribution of the Ag^+ ion and the AgOH(aq) and $Ag(OH)_2^-$ complexes were never found to account for significant proportions of the measured silver concentration at any temperature and pressure. Accordingly, the dissolution of silver sulphide in dilute sulphide solutions in the $pH_{T,P}$ range 3.7 to 12.7 are accurately described by the reactions

$$0.5Ag_2S(s) + 0.5H_2S(aq) = AgHS(aq) \quad K_{s,111} \quad (18)$$

$$0.5Ag_2S(s) + 0.5H_2S(aq) + HS^- = Ag(HS)_2^- \quad K_{s,122} \quad (19)$$

$$Ag_2S(s) + 2HS^- = Ag_2S(HS)_2^{2-} \quad K_{s,232} \quad (20)$$

The solubility constants, $K_{s,111}$, $K_{s,122}$, and $K_{s,232}$, obtained by nonlinear least squares treatment of the all the data at a given temperature and pressure, are given in Table 2 and plotted as a function of temperature in Figures 3 to 5. The uncertainties in the solubility constants represent the one standard error (1σ) of the fit, assuming 5 and 8% uncertainty on measured silver concentrations above and below 1.0×10^{-6} mol kg^{-1} and 3% uncertainties on total sulphide and sodium concentrations, these corresponding to the accuracy of the analysis.

The solubility constant with respect to AgHS(aq) is independent of temperature from 25 to 300°C, varying from $\log K_{s,111}$ = −5.79 (±0.07) to −5.59 (±0.09), and decreases to −5.92

Table 2. Solubility constants $K_{s,111}$, $K_{s,122}$, and $K_{s,232}$ for the AgHS(aq), $Ag(HS)_2^-$ and $Ag_2S(HS)_2^{2-}$ species, respectively, as a function of temperature and pressure. The uncertainties are 1σ.

t/°C	$\log K_{s,111}$		$\log K_{s,122}$		$\log K_{s,232}$	
	swvp	500 bar	swvp	500 bar	swvp	500 bar
25	−5.62 ± 0.04	—	−3.97 ± 0.04	—	−4.78 ± 0.04	—
50	−5.75 ± 0.13	—	−3.75 ± 0.03	—	−4.71 ± 0.11	—
100	−5.69 ± 0.06	−5.66 ± 0.09	−3.34 ± 0.05	−3.44 ± 0.06	−4.75 ± 0.09	−4.67 ± 0.09
150	−5.67 ± 0.07	−5.79 ± 0.07	−3.03 ± 0.05	−3.10 ± 0.07	−4.70 ± 0.11	−4.65 ± 0.10
200	−5.69 ± 0.06	−5.59 ± 0.09	−2.65 ± 0.05	−2.73 ± 0.09	−4.60 ± 0.15	−4.57 ± 0.18
250	−5.69 ± 0.07	−5.74 ± 0.08	−2.49 ± 0.04	−2.53 ± 0.07	—	—
300	−5.72 ± 0.18	−5.75 ± 0.12	−2.28 ± 0.02	−2.29 ± 0.05	—	—
350	−5.83 ± 0.06	−5.78 ± 0.08	−2.12 ± 0.04	−2.10 ± 0.06	—	—
400	—	−5.92 ± 0.16	—	−1.89 ± 0.03	—	—

swvp = saturated water vapour pressure.

Fig. 3. The logarithm of the solubility constant, $\log K_{s,111}$, as a function of temperature at saturated water vapour pressure (swvp) and 500 bar. The line represents the fit to all the data points (Table 3).
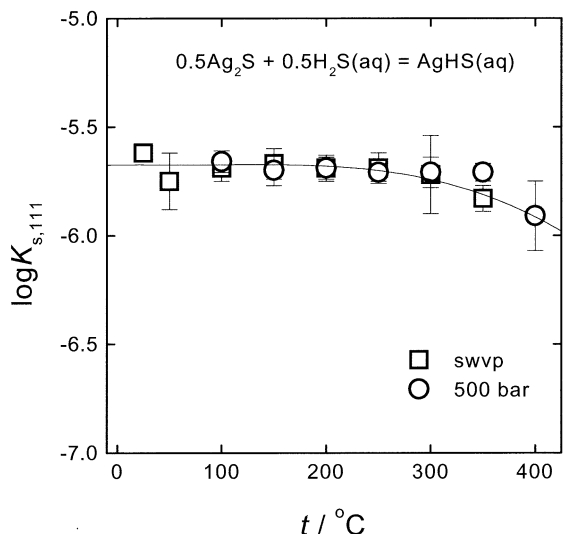

Fig. 5. The logarithm of the solubility constant, $\log K_{s,232}$, as a function of temperature at saturated water vapour pressure (swvp) and 500 bar. The line represents the fit through all the data points (Table 3).

(±0.16) at 400°C. The solubility constant with respect to $Ag(HS)_2^-$ increases with inverse temperature from $\log K_{s,122} = -3.97$ (±0.04) at 25°C to -1.89 (±0.03) at 400°C. The solubility constant with respect to $Ag_2S(HS)_2^{2-}$ increases with increasing temperature from $\log K_{s,232} = -4.78$ (±0.04) at 25°C to -4.57 (±0.18) at 200°C. The equilibrium constants were observed to be independent of pressure within the reported uncertainties. However, the range of pressures studied was small, that is, 490 bar at 100°C and 300 bar at 350°C.

Two static experiments using a silica glass flask (black painted) were conducted at 25°C to confirm that the measured solubilities using the flow-through autoclave truly represented equilibrium solubility. The results of the two different experi-

mental approaches are in good agreement. For the static experiments the solubilities, measured as total dissolved silver, were 6.23×10^{-7} and 4.90×10^{-7} mol kg^{-1} in solutions of total reduced sulphur of 0.061 and 0.048 mol kg^{-1}, respectively. The solubilities using the flow-through apparatus were 4.97×10^{-7} mol kg^{-1} in solutions of total sulphide of 0.053 mol kg^{-1}.

With increasing temperature, the stability field of $Ag(HS)_2^-$ increases and shifts to more alkaline pH in accordance with the shift of the first ionisation constant of $H_2S(aq)$ (Figs. 6 to 8). Consequently, $Ag(HS)_2^-$ is the predominant complex in neutral to alkaline solutions at $t > 200$°C, whereas $Ag_2S(HS)_2^{2-}$ is not an important species. Therefore, the stability of $Ag_2S(HS)_2^{2-}$ could not be determined form our solubility measurements above 200°C.

Three polymorphs of silver sulphide exist. The stable form at low temperature is acanthite, which is monoclinic. Between 176.3 and 177.8°C, acanthite inverts to argentite, which is a body-centered cubic. Between 586 and 622°C, the $Ag_2S(s)$ body-centered cubic form is inverted to a face-centered cubic $Ag_2S(s)$ (Barton, 1980). The measured enthalpies of transition are $\Delta H^\circ_{transition} = +3.98$ and $+2.5$ kJ mol^{-1} (Barton, 1980). The estimated entropies of transition are $\Delta S^\circ_{transition} = +8.8$ and $+6.0$ J mol^{-1} K^{-1}, respectively (Helgeson et al., 1978), assuming Gibbs free energy of transition to be zero, i.e., $\Delta G^\circ_{transition} = 0$. These transitions will therefore have little influence on the values for the solubility constants, i.e., $\Delta G^\circ_{transition}/-RT\ln(10) = \log K_{transition} = 0$.

To generate smooth solubility curves as a function of temperature, the values for the solubility constants in Table 2 were fitted against temperature to a number of equations of the type

$$\log K = A + BT + CT^2 + D/T + E \log T \qquad (21)$$

where T is in Kelvins. The form of Eqn. 21, which best described the temperature variations of each solubility constant using the fewest number of parameters, was selected. The coefficients and the forms of the equations are given in Table 3.
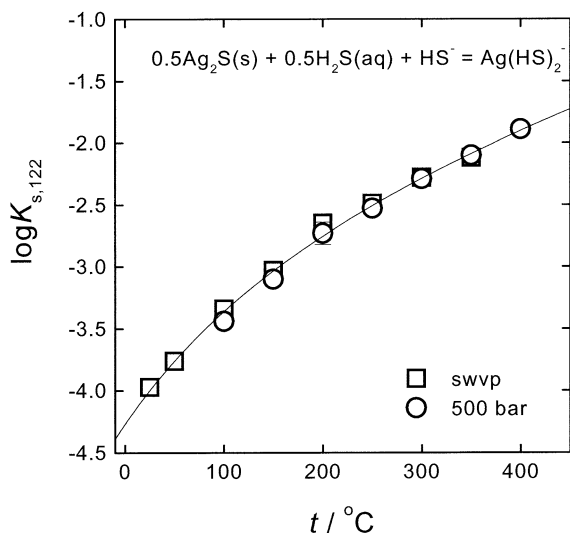

Fig. 4. The logarithm of the solubility constant, $\log K_{s,122}$, as a function of temperature at saturated water vapour pressure (swvp) and 500 bar. The line represents the fit to all the data points (Table 3).
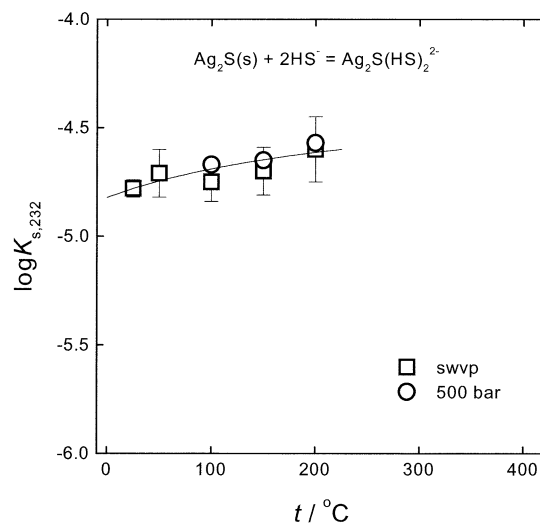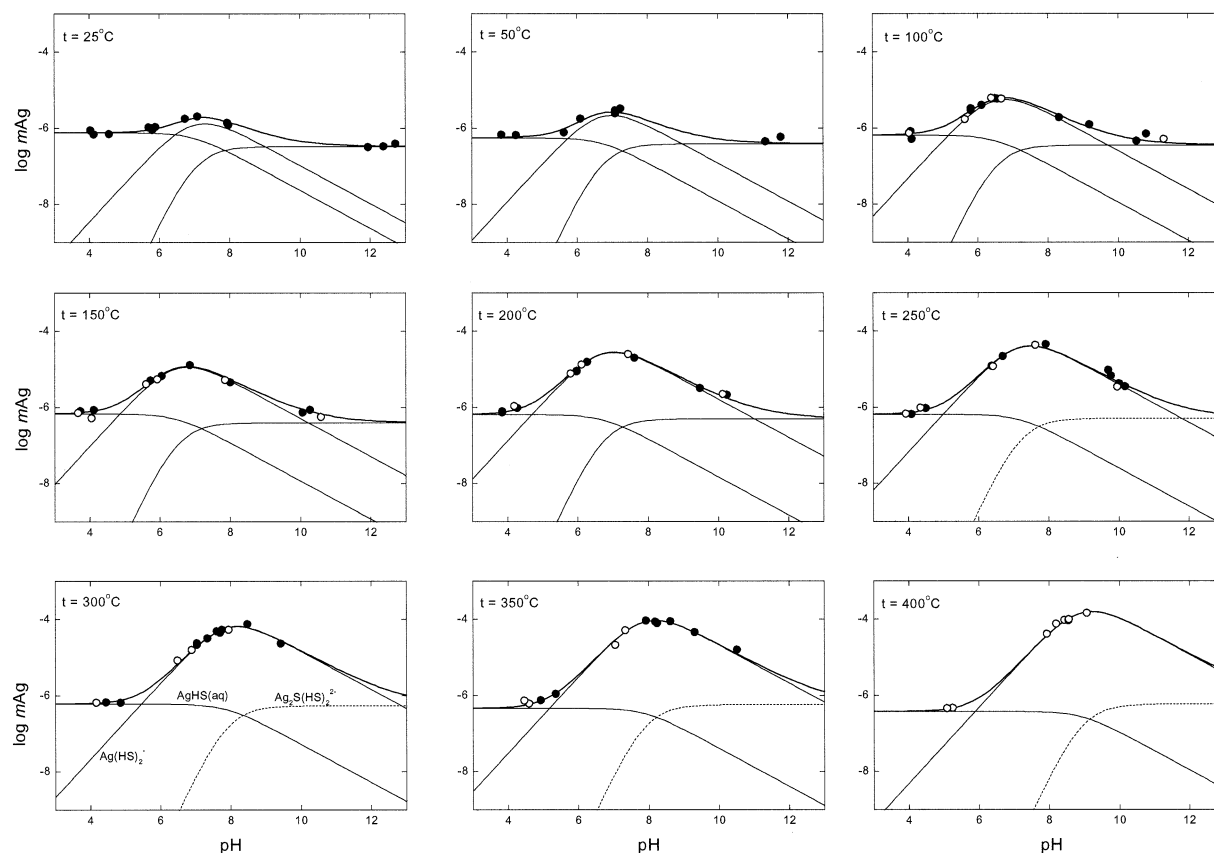
Fig. 6. The solubility of silver sulphide as a function of pH at $mS_{total} = 0.10$ mol kg^{-1}. The data points show the measured solubilities at the experimental pH normalised to constant $mS_{total} = 0.10$ mol kg^{-1}. Filled circles represent data at saturated water vapour pressure and open circles data at 500 bar. The solid curves were calculated from solubility constants given in Table 2 except with respect to $Ag_2S(HS)_2^{2-}$ at $t > 200°C$ (dotted curves) that were calculated by extrapolation of the respective function given in Table 3.

In Figure 6, the calculated solubility curves for silver sulphide in aqueous solutions of $mS_{total} = 0.01$ mol kg^{-1}, using the solubility constants given in Table 2, are compared with the measured solubilities normalised to the same total reduced sulphur concentration. The formation of $Ag_2S(HS)_2^{2-}$ could be experimentally determined only to 200°C. Therefore, the solubility with respect to $Ag_2S(HS)_2^{2-}$ at $t > 200°C$ in Figure 6 was calculated by extrapolating the function given in Table 3. As indicated, good agreement is observed at all temperatures. As seen in Figure 6, AgHS(aq) is the dominant complex stoichiometry under acidic conditions, whereas $Ag(HS)_2^-$ predominates at neutral pH and $Ag_2S(HS)_2^{2-}$ in alkaline solutions. As seen in Figures 3 and 5, the equilibrium solubility constants with respect to AgHS(aq) and $Ag_2S(HS)_2^{2-}$ vary little with temperature, whereas the equilibrium formation constant for $Ag(HS)_2^-$ increases dramatically with increasing temperature. This is accompanied by a shift of the stability field of $Ag(HS)_2^-$ to more alkaline conditions in accordance with the shift of the first ionisation constant of $H_2S(aq)$ (Fig. 7) to smaller values. As a consequence, the stability field of $Ag(HS)_2^-$ increases with increasing temperature and at high temperature this complex dominates at pH>4, whereas $Ag_2S(HS)_2^{2-}$ predominates at pH>10 below 100°C but is unimportant at $t > 200°C$. The stability field of the predominant complex also depends on the

total reduced sulphur concentration, as shown in Figure 8. At low temperatures and low total reduced sulphur concentrations ($mS_{total} < 0.01$ mol kg^{-1}), AuHS(aq) will predominate up to pH = 10, whereas at higher total reduced sulphur concentration, $Ag(HS)_2^-$ and $Ag_2S(HS)_2^{2-}$ become the dominant stoichiometries in neutral and alkaline solutions at $t < 200°C$ and $Ag(HS)_2^-$ at pH>4 above 200°C. However, at temperatures above 300°C, $Ag(HS)_2^-$ predominates at pH>4 and mS_{total} >0.005 mol kg^{-1}, whereas AgHS(aq) predominates at very low total reduced sulphur concentrations.

4.3. Stepwise and Cumulative Formation Constants

The solubility product of silver sulphide, $Ag_2S(s)$

$$0.5Ag_2S(s) + H^+ = Ag^+ + 0.5H_2S(aq) \qquad K_{s,0} \quad (22)$$
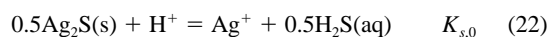
was estimated in the present study from the thermodynamic properties of the aqueous species and the mineral. The results are given in Table 4. The Gibbs free energy of $H_2S(aq)$ was calculated from the experimentally determined Henry's law constant of H_2S (Suleimenov and Krupp, 1994) and the thermodynamic properties of $H_2S(g)$ (Robie et al., 1979). The Gibbs free energy of Ag^+ was calculated from the AgCl(s)
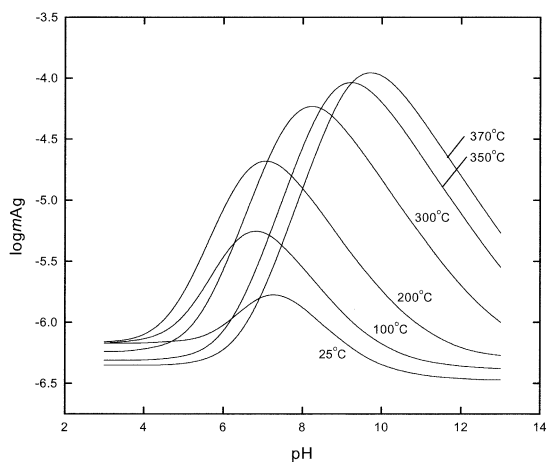
Fig. 7. The solubility of silver sulphide as a function of temperature at saturated water vapour pressure and $mS_{total} = 0.10$ mol kg^{-1} calculated from smooth solubility constants (Table 3). At low temperature, AgHS(aq), $Ag(HS)_2^-$, and $Ag_2S(HS)_2^{2-}$ predominate in acidic, neutral, and alkaline solutions, respectively. With increasing temperature, the stability of $Ag(HS)_2^-$ increases considerably. The maximum solubility occurs where pH equals the first ionisation constant of $H_2S(aq)$. Thus, the stability field of $Ag(HS)_2^-$ is shifted to more alkaline pH values above 200°C in accordance with the shift of the first ionisation constant of $H_2S(aq)$ to smaller values. Consequently, $Ag_2S(HS)_2^{2-}$ predominates in even more alkaline solutions at high temperatures.

solubility measurements (Seward, 1976), the Gibbs free energy of aqueous Cl^- (Cox et al., 1989) and AgCl(s) (Robie et al., 1979).

The cumulative formation constants according to the reactions

$$Ag^+ + HS^- = AgHS(aq) \qquad \beta_{111}, \qquad (23)$$

$$Ag^+ + 2HS^- = Ag(HS)_2^- \qquad \beta_{122}, \qquad (24)$$

$$2Ag^+ + 3HS^- = Ag_2S(HS)_2^{2-} + \quad H^+\beta_{232}, \qquad (25)$$
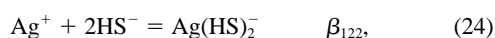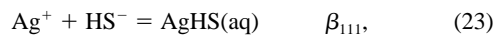
were subsequently calculated from the solubility product of silver sulphide $K_{s,0}$ (Table 4), first ionisation constant of $H_2S(aq)$ (Suleimenov and Seward, 1997) (Appendix B), and the solubility constants $K_{s,111}$, $K_{s,112}$ and $K_{s,232}$ determined in the present study (Table 2) to 350°C at saturated water vapour pressure. From the cumulative formation constants, the stepwise formation constants

$$AgHS(aq) + HS^- = Ag(HS)_2^- \qquad K_{122} \qquad (26)$$

$$Ag_2S(HS)_2^{2-} + HS^- + H^+ = 2Ag(HS)_2^- \qquad K_{232} \qquad (27)$$
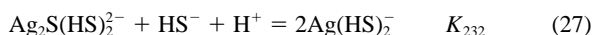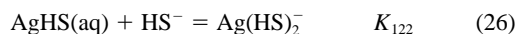
were calculated. The values for the cumulative and stepwise formation constants are given in Table 4.

The logarithms of the values of the stepwise and cumulative formation constants were fitted to various forms of Eqn. 21. The results are given in Table 5. The calculated values and the fitted curves are compared in Figure 9.

It has been demonstrated that the stability constants of the complexes of one d^{10} metal cation vary linearly with another d^{10} cation (Hancock et al., 1977; Renders and Seward, 1989). Such a linear relationship between silver(I) and copper(I) com-
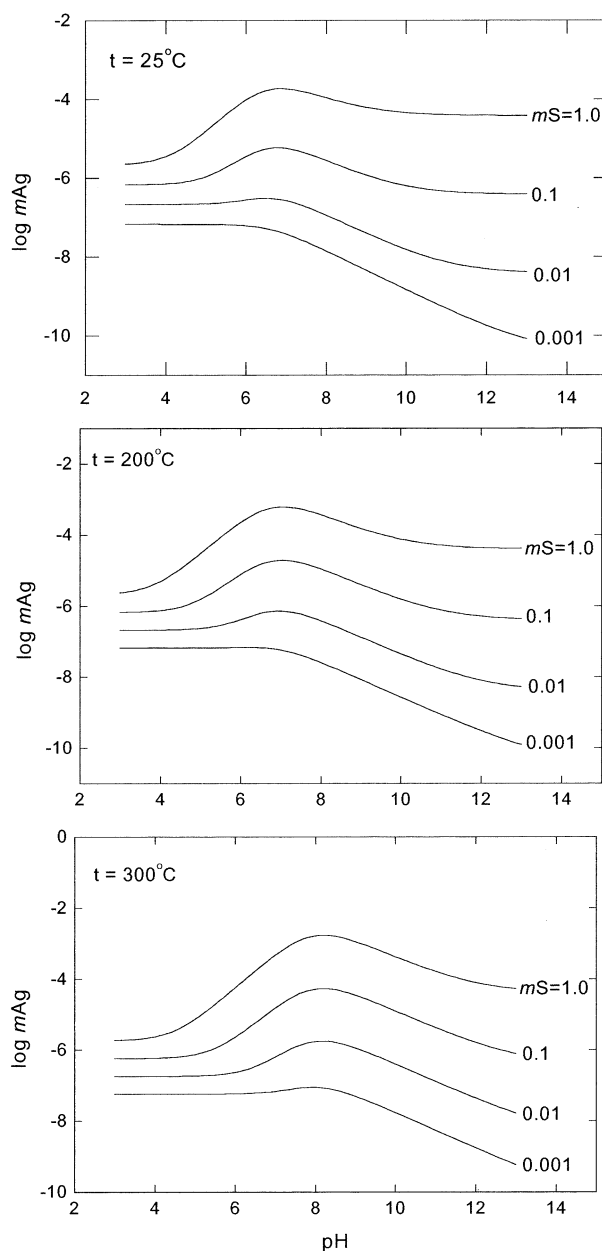
Fig. 8. The solubility of silver sulphide as a function of temperature and total reduced sulphur at 100, 200 and 300°C and saturated water vapour pressure. The curves were calculated from the smoothed solubility constants (Table 3). At low sulphur concentration and all temperatures, AgHS(aq) predominates over the entire pH range. With increasing sulphur concentration, the importance of $Ag(HS)_2^-$ and $Ag_2S(HS)_2^{2-}$ increases. The same is true for the former complex with increasing temperature, whereas the latter becomes unimportant above 200°C.

plexes on one hand and gold(I) complexes on the other is shown in Figure 10. Further, the $Cu(HS)_2^-$, $Ag(HS)_2^-$, and $Au(HS)_2^-$ complex stabilities follow closely this linear trend, and the constants for AgHS(aq) and AuHS(aq) and $Ag_2S(HS)_2^{2-}$ and $Cu_2S(HS)_2^{2-}$ are very close to the linear relationship between silver, gold, and copper complexes stabilities.

Table 3. Coefficients describing the temperature variation of the silver sulphide solubility constants.

	$\log K = A + BT + CT^2 + D/T + E \log T$				
	A	B	C	D	E
$\log K_{s,111}$	54.852	0.033140	$-1.5990\text{E-}05$	-1285.80	-26.136
$\log K_{s,122}$	-2.1714	0.001993		-721.531	
$\log K_{s,232}$	-4.3297			-134.488	

Differentiation of the constants β_{111} and K_{122} yields the enthalpy change for AgHS(aq) and Ag(HS)$_2^-$ and, together with the Gibbs free energy of reaction, the entropy change. The values of ΔG_r^0, ΔH_r^0, and ΔS_r^0 to 350°C at saturated water vapour pressure are summarised in Table 6. The interaction of Ag$^+$ with HS$^-$ ligands can be classified as a typical soft-soft ion-ligand reaction. Such reactions are often characterised by exothermic enthalpies and small entropy changes, as the energy required to replace a water molecule for a ligand is less than the energy gained by the complex formation. Indeed, the formation of AgHS(aq) at 25°C is accompanied by a negative enthalpy and a small negative entropy, suggesting that the interaction between Ag$^+$ and HS$^-$ is predominantly covalent. With increasing temperature to 200°C, the enthalpy of reaction is close to constant. Above 200°C, the reaction becomes endothermic, accompanied by a large positive entropy, suggesting that the interaction between Ag$^+$ and HS$^-$ at high temperatures is increasingly electrostatic. A similar behavior has been observed for other aqueous d^{10} systems in our laboratory, such as for gold(I) hydrosulphide complexes and silver(I) chloride complexes (Seward, 1976). The second stepwise addition of HS$^-$ to form Ag(HS)$_2^-$ is more electrostatic at all temperatures.

4.4. Comparison With Previous Results

Treadwell and Hepenstick (1949) measured the solubility of acanthite at 20°C to pH of 7. Their results indicate that the solubility is pH independent under acidic conditions, whereas it increases dramatically at neutral pH. Treadwell and Hepenstick (1949) concluded that AgHS(aq) predominates in acidic solutions but were unable to interpret the results at neutral pH because of oxidation of H$_2$S in the experiments. However, their solubilities in acidic solutions with respect to AgHS(aq) are very similar to the one obtained in this study.

Schwarzenbach et al. (1958) measured the solubility of fresh silver sulphide in aqueous sulphide solutions at 25°C. Later, Schwarzenbach and Widmer (1966) measured the solubility of

freshly precipitated silver sulphide in aqueous sulphide solutions at constant ionic strength of 1 mol kg^{-1} NaClO$_4$ at 20°C. They interpreted their results with respect to AgHS(aq), Ag(HS)$_2^-$ and Ag$_2$S(HS)$_2^{2-}$ and reported solubility constants with the respective complexes. Schwarzenbach et al. (1958) and Schwarzenbach and Widmer (1966) obtained much lower solubilities in acidic solutions compared to the present results. The reason for this is unclear. However, our experimental results in acidic sulphide solutions using both the flow-though autoclave system and a static, black-coloured, silica glass reaction vessel are in good agreement. In both cases, well-crystallised silver sulphide was used, and care was taken to prevent photoreduction of silver sulphide to elemental silver as well as to eliminate any air contamination. However, Schwarzenbach et al. (1958) and Schwarzenbach and Widmer (1966) precipitated the silver sulphide in situ, which would result in very fine-grained material, and did not report if the experiments were conducted in the dark and without any possible air contamination. With respect to the Ag(HS)$_2^-$ complex, the equilibrium solubility constants obtained at 20°C of $\log K_{s,122} = -4.05$ in the present study is practically the same as the one obtained by Schwarzenbach and Widmer (1966) of -4.02 at zero ionic strength. The same is true for the solubility constant with respect to Ag$_2$S(HS)$_2^{2-}$ of $\log K_{s,232} = -4.79$ obtained in the present study at 20°C compared to -4.82 by Schwarzenbach and Widmer (1966) at zero ionic strength.

Melent'yev et al. (1969) measured the solubility of silver sulphide in the temperature range 100 to 180°C at pH 1.2 to 7.9. They did not, however, determine the dominant silver(I) sulphide complex stoichiometry or stability. The narrow range in total sulphide and pH does not allow for independent determination of silver(I) sulphide complex stoichiometry and stability. However, at pH <3, it is evident from the results of Melent'yev et al. (1969) that the solubility increases with decreasing pH, indicating a positively charged species under these conditions. According to the solubility product of silver sulphide estimated

Table 4. Cumulative and stepwise formation constants of aqueous silver(I) sulphide complexes as a function of temperature at saturated water vapour pressure.

t/°C	$\log K_{s,0}$	$\log \beta_{111}$	$\log \beta_{122}$	$\log \beta_{232}$	$\log K_{122}$	$\log K_{232}$
25	-14.52	15.89	17.54	31.24	1.65	3.83
50	-13.16	14.16	16.15	25.65	1.99	6.64
100	-10.89	11.69	14.04	23.52	2.35	4.56
150	-9.11	9.93	12.57	20.01	2.64	5.13
200	-7.73	8.77	11.81	17.58	3.04	6.03
250	-6.66	8.16	11.36		3.20	
300	-5.83	8.00	11.44		3.44	
350	-5.15	8.21	11.92		3.71	

Table 5. Coefficients describing the temperature variation of the solubility product of silver sulphide and cumulative and stepwise formation constants.

	$\log K, \beta = A + BT + CT^2 + D/T + E \log T$				
	A	B	C	D	E
$\log K_{s,0}$	3.62418	—	—	−5408.09	—
$\log \beta_{111}$	4.01234	−0.03809	4.8671E-05	5628.59	—
$\log \beta_{122}$	12.37382	−0.04714	5.7032E-05	4217.81	—
$\log \beta_{232}$	−34.36551	0.04005	—	15736.24	—
$\log K_{122}$ [a]	8.36147	−0.00905	8.3607E-06	−1410.78	—
$\log K_{232}$ [b]	59.11314	−0.13433	1.1406E-04	−7300.62	—

[a] $\log K_{122} = \log \beta_{122} - \log \beta_{111}$
[b] $\log K_{232} = 2 \log \beta_{122} - \log \beta_{232}$

in this study (Table 4), the Ag^+ cannot account for this increased solubility. As pointed out by Gammons and Barnes (1989), this behavior is possibly due to a charged complex of the form $Ag(H_2S)_n^+$. However, using the same speciation scheme as in the present study, it is evident that the measured solubility data of Melent'yev et al. (1969) are in good agreement with the present study with respect to AgHS(aq) and $Ag(HS)_2^-$.

Wood et al. (1987) measured the solubility of the assemblage pyrite + pyrrhotite + magnetite + sphalerite + galena + argentite + gold + stibnite + bismuthinite + molybdenite between 200 and 350°C in aqueous acidic solutions containing up to 5.0 m NaCl. They were unable to estimate the complex stoichiometry and stability because of narrow pH and total sulphur range and overall complexity of the system.

Sugaki et al. (1987) measured the solubility of silver sulphide between 25 and 250°C with pH (at 25°C) ranging from 3.5 to 11. They interpreted their results in terms of dinuclear silver(I) sulphide complexes of the form $Ag_2S(H_2S)(aq)$, $Ag_2S(H_2S)(HS)^-$, $Ag_2S(H_2S)(HS)_2^{2-}$, and $Ag_2S(HS)_2^{2-}$. They

did not consider mononuclear nor polynuclear complexes of higher order than two. However, their data are very scattered at all temperatures, making any conclusive results on either stoichiometry or stability of silver(I) sulphide complexes impossible.

Gammons and Barnes (1989) determined the solubility of silver sulphide at 25 to 300°C and pH and total reduced sulphur between 5.8 and 7.3 and 0.2 and 1.4 mol kg^{-1}, respectively. They concluded that under these conditions, $Ag(HS)_2^-$ is the dominant stoichiometry and calculated the equilibrium solubility constants with respect to this species. The calculated solubility constants of Gammons and Barnes (1989) carry some inherent uncertainties at all temperatures due to large scatter of their solubility data. Despite the considerable scatter, however, their values for $K_{s,122}$ are in reasonably good agreement with our data up to 150°C at saturated water vapour pressure, whereas above 150°C, the equilibrium constants obtained in this study with respect to $Ag(HS)_2^-$ are systematically lower by 0.1 to 0.2 log units than those reported by Gammons and Barnes (1989). However, agreement with their values of $K_{s,122}$ at 25°C is possibly fortuitous, given that their measured solubilities at this temperature were also due to the presence of AgHS(aq) and $Ag_2S(HS)_2^{2-}$ as well as to $Ag(HS)_2^-$.

5. AQUEOUS SPECIATION AND TRANSPORT OF SILVER BY HYDROTHERMAL SOLUTIONS

5.1. Speciation of Silver in Aqueous Solutions

The percentage distribution of silver(I) complexes in solution as a function of solution composition and temperature is shown in Figure 11. The data required to calculate the various parts of Figure 11 are from Seward (1976), Zotov et al. (1982), Kozlov et al. (1983), Kozlov (1985), and the current study. The solution compositions used for these calculations are those typically found in natural environments and for 0.5 mol kg^{-1} dissolved sulphide and chloride. In dilute, H_2S free solution at 25°C, the free Ag^+ ion and mixed $AgClOH^-$ complex predominate below and above pH 3, respectively (Fig. 11a). In deep anoxic seawater (Fig. 11b) and high chloride and high sulphide water (Fig. 11c) at 25°C, silver(I) sulphide complexes predominate under all pH conditions. For dilute low-temperature geothermal waters at 100°C, the free Ag^+ ion dominates at pH<4.5, whereas the mixed $AgClOH^-$ complex becomes the most important one at pH>4.5 (Fig. 11d). For low-temperature
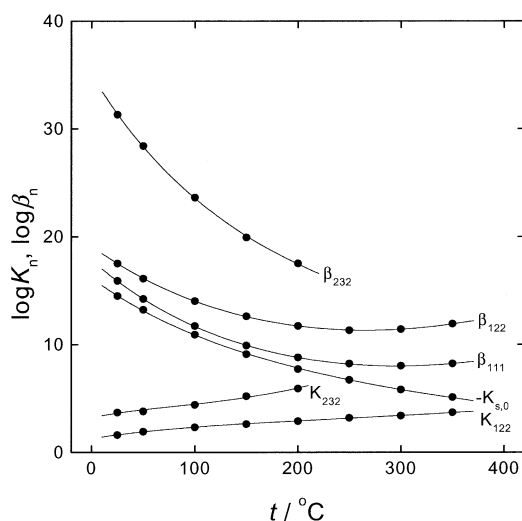
Fig. 9. The logarithm of the stepwise and cumulative formation constants and the solubility product of silver sulphide as a function of temperature at saturated water vapour pressure. The closed circles represent the experimentally determined values (Table 5), and the curves are the fits through the data points (Table 6).
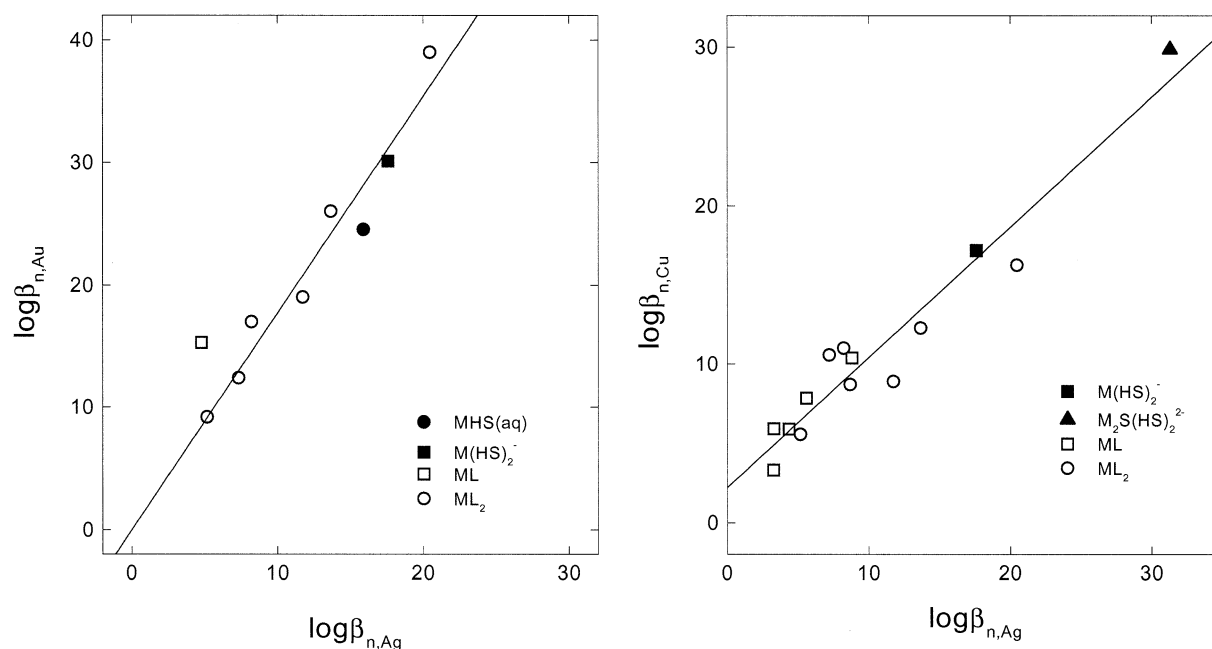
Fig. 10. The relationship between the stability constants of copper(I), silver(I) and gold(I) at 25°C and 1 bar containing one and two ligands (L = Cl$^-$, Br$^-$, I$^-$, SO$_3^{2-}$, SCN$^-$, CN$^-$, NH$_3$, S$_2$O$_3^{2-}$) including hydrosulphide and sulphide. The plots are based on data from this study (Table 5) as well as from Berne and Leden (1953), Lieser (1957), Connick and Paul (1961), Hopkins and Wunlft (1965), Jørgenson and Pouradier (1970), Peshchevitsky et al. (1970), Martell and Smith (1989), Renders and Seward (1989), Xiao et al. (1998), and Mountain and Seward (1999).

geothermal fluids of seawater salinity at 100°C, the picture is more complex (Fig. 11e). At pH<3, the silver(I) chloride complexes dominate, whereas AgHS(aq) is the most important complex in neutral solutions and AgClOH$^-$ in alkaline solutions. At high chloride and sulphide concentration and 100°C, silver(I) sulphide complexes dominate under all pH conditions (Fig. 11f). For dilute geothermal fluids at 300°C, AgCl(aq) predominates under acidic conditions, whereas silver(I) sulphide complexes predominate in slightly acidic to alkaline fluids (Fig. 11g). For the high-temperature geothermal seawater at 300°C, the AgCl$_2^-$ species dominates to pH 8, whereas in alkaline solutions, the AgClOH$^-$ complex is the most important (Fig. 11h). At high chloride and sulphide concentrations, AgCl$_2^-$ and Ag(HS)$_2^-$ are the most important species below and above pH 5, respectively (Fig. 11i). It is therefore clear that the dominant silver(I) species in solution are extremely dependent

on temperature and fluid composition. In dilute solution at low temperatures, the Ag$^+$ and AgClOH$^-$ species predominate. With increasing temperature and salinity, the silver(I) chloride complexes become important. However, in sulphide-containing solutions at all temperatures and chloride concentrations up to 0.5 mol kg^{-1}, silver(I) sulphide complexes are most important.

5.2. Transport of Silver by Hydrothermal Fluids

Hydrothermal silver ore deposits are formed when silver complexes, transported by the fluid, become unstable. Changes in temperature, pressure, ligand activity, phase separation, boiling, mixing, and mineral precipitation can lead to the instability of aqueous silver complexes and loss from the fluid, with the dominant silver complexes being defined by the fluid's composition, temperature, and pressure.

Table 6. The thermodynamic properties for the stepwise formation of AgHS(aq) and Ag(HS)$_2^-$ to 350°C at saturated water vapour pressure, calculated from coefficients given in Table 5.

t/°C	ΔG_r^0/kJ mol^{-1}		ΔH_r^0/kJ mol^{-1}		ΔS_r^0/J mol^{-1} K^{-1}	
	AgHS(aq)	Ag(HS)$_2^-$	AgHS(aq)	Ag(HS)$_2^-$	AgHS(aq)	Ag(HS)$_2^-$
25	−90.5	−9.6	−123.2	20.1	−109	99
50	−87.9	−12.0	−121.0	19.7	−103	98
100	−83.3	−16.9	−112.5	19.5	−78	98
150	−80.3	−21.8	−97.1	20.2	−40	99
200	−79.6	−26.9	−73.6	22.1	13	104
250	−81.8	−32.2	−40.5	25.4	79	110
300	−87.7	−37.9	3.6	30.3	159	119
350	−98.0	−44.2	60.1	37.2	254	131

Fig. 11. The percentage distribution of silver(I) species as a function of solution composition and temperature. (a) Average river water composition of $mS_{total} = 0.0$ and $mCl_{total} = 1.6 \times 10^{-4}$ at 25°C (Martin and Whitfield, 1983). (b) Deep anoxic seawater $mS_{total} = 5.0 \times 10^{-4}$ and $mCl_{total} = 0.55$ at 25°C (Haraldsson and Westerlund, 1988; Hastings and Emerson, 1988; Dyrssen and Kremling, 1990). (d) Typical dilute low-temperature geothermal water in Iceland with $mS_{total} = 0.0$ and $mCl_{total} = 0.001$ at 100°C (Arnórsson, 1995). (e) Low-temperature hydrothermal fluids of seawater salinity with $mS_{total} = 1.0 \times 10^{-4}$ and $mCl_{total} = 0.5$ at 100°C. (g) Dilute natural high-temperature geothermal water at Ohaaki-Broadlands with $mS_{total} = 0.004$ and $mCl_{total} = 0.03$ at 300°C (Mahon and Finlayson, 1972; DSIR files). (h) High-temperature geothermal seawater at Reykjanes, Iceland, with $mS_{total} = 5.0 \times 10^{-4}$ and $mCl_{total} = 0.61$ at 300°C (Arnórsson et al., 1983). (c), (f), and (i) 0.5 mol kg^{-1} H$_2$S and Cl solution at 25, 100 and 300°C, respectively. The shaded areas represent typical pH values found for the respective water type at aquifer temperature. The complex stabilities used for these calculations are based on experimental data on silver(I) sulphide complexes obtained in this study (Table 3), silver(I) chloride complexes (Seward, 1976), hydroxide complexes (Kozlov et al., 1983), mixed hydroxychlorido complexes (Zotov et al., 1982), and carbonate and hydroxycarbonate complexes (Kozlov, 1985).

Many active geothermal systems can be viewed as modern analogs of epithermal ore-depositing environments. By studying such systems, quantitative information can be obtained on the fundamental processes controlling the transport and depositional mechanisms of precious metals such as silver and gold. Examples of active ore-forming geothermal systems are the Ohaaki-Broadlands and Rotokawa geothermal systems, New Zealand (Weissberg et al., 1979; Brown, 1986; Krupp and Seward, 1987), the geothermal seawater system at Reykjanes, Iceland (Hardardóttir et al., 2001), the Salton Sea, California (e.g., McKibben et al., 1988), and Cerro Prieto, Mexico (Clark and Williams-Jones, 1990). Silicate and sulphide scales are common in pipelines at Reykjanes, these containing up to 93 and over 400 ppm gold and silver, respectively (Hardardóttir et al., 2001). At Rotokawa, sulphide minerals such as argentite have been identified at depth and at the surface, sulphide rich muds have been analysed and found to contain up to 50 and 10 ppm gold and silver, respectively (Krupp and Seward, 1987). At Ohaaki-Broadlands, very high concentrations of silver and gold of up to 25.7 and 7.1 wt.%, respectively, have been reported in deposits on the downstream side of orifice (pressure release) plates in the production pipelines (Brown, 1986). It is therefore clear that the fluids can transport considerable amount of silver.

Table 7. Compositions of aquifer fluids at Ohaaki-Broadlands (BR), New Zealand, and Reykjanes (REK), Iceland, measured and calculated silver concentration of the aquifer fluid and silver speciation.

	BR 22 (Well 22)	BR 9 (Well 9)	BR 20 (Well 20)	REK (Well 8)
Composition[a]/(ppm)				
t/°C	271[b]	289[b]	298[b]	244[c]
pH_T	6.22	6.07	5.96	5.40
SiO_2	560	633	667	582
B	33	39	36	8.00
Na	961	744	738	10276
K	149	157	151	1585
Ca	1.0	3.6	2.2	1571
Mg	0.08	0.27	0.02	1.33
ΣCO_2	4956	9815	17720	466
ΣSO_4	1.6	3.7	9.8	26.2
H_2S	123	136	190	15.7
Cl	1138	1308	1239	21045
Measured $m\ Ag_{total}$/ppb	8[d]	12.7 to 18.9[e]	5.74 to 12.15[e]	n.a.
Calculated $m\ Ag_{total}$/ppb	17[f]	15[f]	18[f]	27
Speciation				
log $m\ Ag^+$	<0.1%	<0.1%	<0.1%	<0.1%
log $m\ AgCl(aq)$	0.2%	<0.1%	1.1%	2.8%
log $m\ AgCl_2^-$	0.4%	1.8%	2.6%	75.9%
log $m\ AgCl_3^{2-}$	<0.1%	<0.1%	<0.1%	11.2%
log $m\ AgCl_4^{3-}$	<0.1%	<0.1%	<0.1%	<0.1%
log $m\ AgHS(aq)$	72.5%	79.9%	79.9%	9.8%
log $m\ Ag(HS)_2^-$	26.9%	17.5%	16.3%	0.2%
log $m\ Ag_2S(HS)_2^{2-}$	<0.1%	<0.1%	<0.1%	<0.1%
log $m\ AgOHCl^-$	<0.1%	<0.1%	<0.1%	<0.2%

[a] The composition of the aquifer fluid was calculated with the aid of the WATCH program (Arnórsson et al., 1982; Bjarnason, 1994) from analysis of water and collected at the well head given by Arnórsson et al. (1983) for Reykjanes and Mahon and Finlayson (1972), and DSIR files for Ohaaki-Broadlands.

[b] Reservoir temperature estimated using the quartz geothermometer (Fournier and Potter, 1982).

[c] Measured temperature.

[d] Minimum number taken from Brown (1986).

[e] Concentration in deep geothermal fluids taken from Brown and Webster (1998).

[f] Calculated total silver in equilibrium with $Ag_2S(s)$.

The fluid chemistry at Ohaaki-Broadlands has been extensively studied (e.g., Mahon and Finlayson, 1972), and analytical data on silver concentration in the aquifer are available for some wells (Brown, 1986; Brown and Webster, 1998). The fluid chemistry with respect to major components at Reykjanes Iceland has been studied by number of authors (e.g., Arnórsson, 1978; Arnórsson et al., 1983; Ragnarsdóttir et al., 1984), but no data are available at present on silver concentration in the aquifer fluids at Reykjanes. These data on fluid compositions allow an assessment of silver transport mechanism by hydrothermal fluids. The aquifer fluid composition and speciation were calculated from analytical data given by Mahon and Finlayson (1972) and New Zealand DSIR file reports as well as by Brown (1986) and Brown and Webster (1998) for the Ohaaki-Broadlands and from Arnórsson et al. (1983) for Reykjanes fluids with the aid of the WATCH computer program (Arnórsson et al., 1982; Bjarnason, 1994). In the present study, a supplement was added to the program to include silver(I) sulphide, chloride, hydroxide, hydroxychloro, carbonate, and hydroxycarbonate complexes using data on complex stability obtained in this study and by Seward (1976), Zotov et al. (1982), Kozlov et al. (1983), and Kozlov (1985).

The aquifer composition measured and calculated silver concentration in the aquifer fluid and the distribution of silver species at Ohaaki-Broadlands and Reykjanes are given in Table 7. As indicated, silver is predominantly present as AgHS(aq) and $Ag(HS)_2^-$ complexes in dilute fluids at Ohaaki-Broadlands, whereas $AgCl_2^-$ is the most important species in geothermal seawater at Reykjanes. A close agreement is obtained between the measured and the calculated silver concentration at Ohaaki-Broadlands assuming that solubility of silver sulphide controls the total silver in solution. Unfortunately there are no data available on the dissolved silver concentration of the aquifer fluids at Reykjanes.

The effect of conductive cooling and closed-system adiabatic boiling on the activity of critical species and transport of silver in the Broadlands-Ohaaki fluids and for the geothermal seawater at Reykjanes, Iceland, assuming equilibrium with silver sulphide are shown in Figures 12 and 13. The calculations were performed using the WATCH program (Arnórsson et al., 1982; Bjarnason, 1994), and the calculation procedure was explained in detail by Arnórsson et al. (1982).

The physical and chemical changes that result from the boiling process and affect silver sulphide saturation include degassing of H_2S and pH increase. pH increases quite drastically during boiling, especially in the early stage because of degassing of CO_2 and to a lesser extent H_2S. Conductive cooling leads to decreasing pH and only minor effects on aqueous species activities.

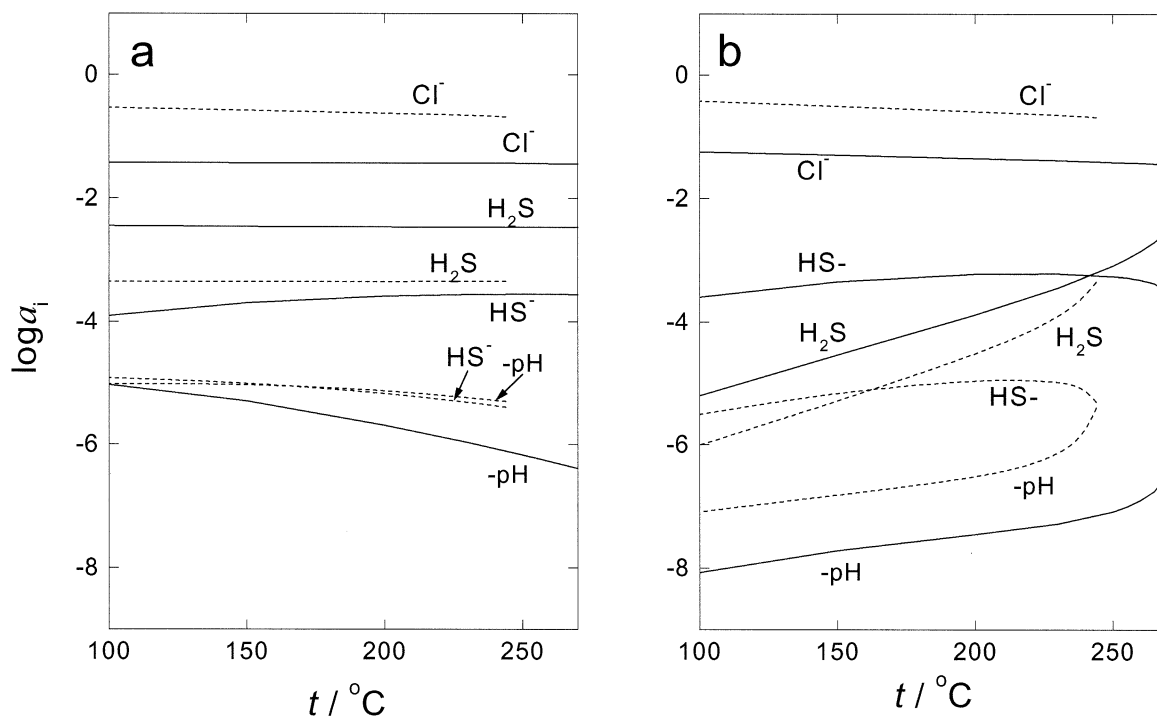Adiabatic boiling of both the geothermal fluids at Ohaaki-

Fig. 12. Effect of (a) conductive cooling (b) and adiabatic boiling on aqueous species distribution for geothermal fluids at Ohaaki-Broadlands, well 22 (solid lines) and Reykjanes, well 8 (dashed lines).

Broadlands and Reykjanes leads to quantitative loss of silver from the fluids and precipitation of silver sulphide. A more rapid loss of silver is indicated for the geothermal seawater at Reykjanes compared to the Ohaaki-Broadlands fluids and oc-

Fig. 13. The effect conductive cooling (dashed lines) and adiabatic boiling (solid lines) on silver concentration assuming that dissolved silver in solution is controlled by silver sulphide solubility. mAg_T/mAg_{inital} is the ratio between equilibrium silver sulphide solubility at a given temperature t and the initial equilibrium solubility at the aquifer fluid temperature.

curs as the dominant silver(I) complexes in solution become unstable. At Reykjanes, silver(I) chloride complexes predominate at aquifer temperatures. Upon adiabatic boiling and cooling, the stabilities of AgCl(aq) and $AgCl_2^-$ decrease dramatically together with H_2S loss, until a plateau is reached at ~150°C, at which the AgHS(aq) complex starts to predominate. On the other hand, AgHS(aq) is the predominant complex in the aquifer fluids at Ohaaki-Broadlands. The loss of silver from these fluids is therefore mainly caused by H_2S loss upon boiling, as observed for sulphide complexes of gold in Ohaaki-Broadlands fluids (Seward, 1989).

For the dilute fluids at Ohaaki-Broadlands, cooling leads to only a minor loss of silver from solution. This can be attributed to the fact that AgHS(aq) makes up 70% of total dissolved silver in the aquifer fluids, and 30% is accounted for by $Ag(HS)_2^-$. The solubility of silver sulphide with respect to AgHS(aq) is almost temperature independent (Fig. 3). The decrease in Ag_2S solubility on cooling (Fig. 13) is thus due to minor changes in pH and the associated change in $Ag(HS)_2^-$ solubility with decreasing temperature (Fig. 4). For the saline aquifer fluids at Reykjanes, the $AgCl_2^-$ complex predominates. The solubility of silver sulphide with respect to $AgCl_2^-$ decreases dramatically with decreasing temperature, and hence, silver is lost from solution upon cooling. At ~175°C, AgHS(aq) becomes the most important complex in solution, and below that temperature, insignificant silver sulphide is precipitated upon cooling (Fig. 3).

6. CONCLUSIONS

The solubility of crystalline silver sulphide was measured in aqueous sulphide solutions as a function of temperature be-
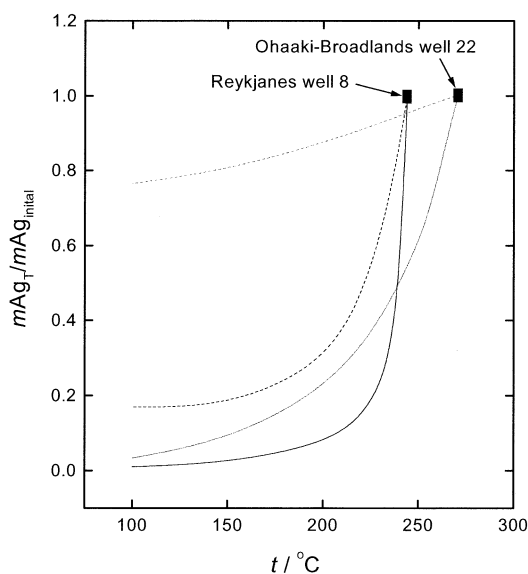
tween 25°C and 400°C and at saturated water vapour pressure and 500 bar. The solubilities, measured as total dissolved silver, were in the range 1.0×10^{-7} to 1.30×10^{-4} mol kg^{-1} (0.01 to 14.0 ppm), in solutions of total reduced sulphur between 0.007 and 0.176 mol kg^{-1} and pH$_{T,P}$ of 3.7 to 12.7. A nonlinear least squares treatment of the data demonstrates that the solubility of silver sulphide in aqueous sulphide solutions of acidic to alkaline pH can be accurately described by three species AgHS(aq), Ag(HS)$_2^-$, and Ag$_2$S(HS)$_2^{2-}$. The solubility constants for AgHS(aq) and Ag$_2$S(HS)$_2^{2-}$ are only weakly dependent on temperature, whereas the solubility with respect to Ag(HS)$_2^-$ increases almost linearly with the inverse of temperature.

The predominant silver(I) species in natural hydrothermal solutions are dependent on temperature and fluid composition. The effects of pressure are minor in the range to 500 bar. In dilute solution at low temperatures, the free Ag$^+$ ion and the mixed ligand species AgClOH$^-$ predominate, whereas with increasing temperature and salinity, the silver(I) chloride complexes become important. However, in sulphide-containing solutions at all temperatures and chloride concentration up to 0.5 mol kg^{-1}, silver(I) sulphide complexes are most important.

Adiabatic boiling of dilute and saline geothermal waters at Ohaaki-Broadlands, New Zealand, and Reykjanes, Iceland, leads to precipitation of silver sulphide and quantitative loss of silver from solution. This is in agreement with the observation of argentite found associated with mineral precipitation in geothermal systems in New Zealand (Krupp and Seward, 1987) and high levels of silver in scale formations at Reykjanes (Hardardóttir et al., 2001). On the other hand, conductive cooling has insignificant effects on silver concentration in dilute fluids, whereas silver is quantitatively lost in geothermal seawater upon cooling.

Associate editor: L. Benning

REFERENCES

Arnórsson S. (1978) Major element chemistry of the geothermal seawater at Reykjanes and Svartsengi, Iceland. *Min. Mag.* **42,** 209–220.

Arnórsson S. (1995) Geothermal systems in Iceland: Structure and conceptual models—II. Low-temperature areas. *Geothermics* **24,** 603–629.

Arnórsson S., Sigurdsson S., and Svavarsson H. (1982) The chemistry of geothermal waters in Iceland. I. Calculation of aqueous speciation from 0° to 370°C. *Geochim. Cosmochim. Acta* **46,** 1513–1532.

Arnórsson S., Gunnlaugsson E., and Svavarsson H. (1983) The chemistry of geothermal waters in Iceland. II. Mineral equilibria and independent variables controlling waters compositions. *Geochim. Cosmochim. Acta* **47,** 547–566.

Barton M. D. (1980) The Ag-Au-S system. *Econ. Geol.* **75,** 303–316.

Berne E. and Leden I. (1953) Die Komplexbildung zwischen Silberionen und Bromidionen in Wässrigen Lösungen. *Z. Naturforschung.* **8a,** 719–726.

Bjarnason J. Ó. (1994) *The Speciation Program WATCH Version 2.1.* Icelandic National Energy Authority.

Brown K. L. (1986) Gold deposition from geothermal discharges in New Zealand. *Econ. Geol.* **81,** 979–983.

Brown K. L. and Webster J. G. (1998) Precious metals in deep geothermal fluids at the Ohaaki geothermal field. In *Water-Rock Interaction 9* (eds. G. B. Arehart and J. R. Hulston), pp. 617–620. Balkema.

Clark J. R. and Williams-Jones A. E. (1990) Analogs of epithermal gold-silver deposition in geothermal well scales. *Nature* **346,** 644–645.

Connick R. E. and Paul A. D. (1961) The fluoride complexes of silver and stannous ions in aqueous solution. *J. Phys. Chem.* **65,** 1216–1220.

Cox J. D., Wagman D. D., and Medvedev V. A. (1989) *CODATA Key Values for Thermodynamics.* Hemisphere, Washington, DC.

Dyrssen D. and Kremling K. (1990) Increasing hydrogen sulphide concentration and trace metal behaviour in the anoxic Baltic waters. *Mar. Chem.* **30,** 193–204.

Ellis A. J. and McFadden I. M. (1972) Partial molal volumes of ions in hydrothermal solutions. *Geochim. Cosmochim. Acta* **36,** 413–426.

Fournier R. O. and Potter R. W. (1982) A revised and expanded silica (quartz) geothermometer. *Geotherm. Res. Con. Bull.* **11,** 3–9.

Gammons C. H. and Barnes H. L. (1989) The solubility of Ag$_2$S in near-neutral aqueous sulfide solutions at 25 to 300°C. *Geochim. Cosmochim. Acta* **53,** 279–290.

Gammons C. H. and Williams-Jones A. E. (1995) The solubility of Au-Ag alloy + AgCl in HCl/NaCl solutions at 300°C: New data on the stability of Au(I) chloride complexes in hydrothermal solutions. *Geochim. Cosmochim. Acta* **59,** 3453–3468.

Hancock R. D., Finkelstein N. P., and Evers A. (1977) A linear free-energy relation involving the formation constants of palladium(II) and platinum(II). *J. Inorg. Nuclear Chem.* **39,** 1031–1034.

Haraldsson C. and Westerlund S. (1988) Trace metals in the water columns of the Black Sea Framvaren Fkord. *Mar. Chem.* **23,** 417–424.

Hardardóttir V., Kristmannsdóttir H., and Ármannsson H. (2001) Scale formation in wells RN-9 and RN-8 in the Reykjanes geothermal field Iceland. In *Water-Rock Interaction 10* (ed. R. Cidu), pp. 851–854. Balkema.

Hastings D. and Emerson S. (1988) Sulfate reduction in the presence of low oxygen levels in the water column of the Cariaco Trench. *Limnol. Oceanogr.* **33,** 391–396.

Helgeson H. C., Delany J. M., Nesbitt H. W., and Bird D. K. (1978) Summary and critique of the thermodynamic properties of rock-forming minerals. *Am. J. Sci.* **278-A,** 1–229.

Helgeson H. C., Kirkham D. H., and Flowers G. C. (1981) Theoritical prediction of the thermodynamic behavior of aqueous electrolytes at high pressures and temperatures: IV. Calculation of activity coefficients, osmotic coefficients and apparent molal and standard and relative partial molal properties to 5 kb and 600°C. *Am. J. Sci.* **281,** 1241–1516.

Hill P. G. (1990) A unified fundamental equation for the thermodynamic properties of H$_2$O. *J. Phys. Chem. Ref. Data* **19,** 1233–1274.

Ho C. P. and Palmer D. A. (1996) Ion association of dilute aqueous sodium hydroxide solutions to 600°C and 300 MPa by conductance measurements. *J. Sol. Chem.* **26,** 711–729.

Ho C. P., Palmer D. A., and Mesmer R. E. (1994) Electrical conductivity measurements of aqueous sodium chloride solutions to 600°C and 300 MPa. *J. Sol. Chem.* **23,** 997–1018.

Hopkins H. P. and Wunlft C. L. (1965) The solution thermochemistry of polyvalent electrolytes. II. Silver sulfate. *J. Phys. Chem.* **69,** 9–11.

Jørgenson C. K. and Pouradier J. (1970) No. 15. Un noveau type de stabilization du "champs de ligands" dans les complexes lineaires du cuivre(I), de l'argent(I), et de l'or(I). *J. Chim. Phys.* **67,** 124–127.

Kielland J. (1937) Individual activity coefficients of ions in aqueous solutions. *J. Am. Chem. Soc.* **59,** 1675–1678.

Kozlov V. K. (1985) Laboratory data on the role of carbonate complexes in hydrothermal silver transport. *Geochem. Intl.* **22,** 85–95.

Kozlov V. K., Kuzenetsov V. N., and Khodakovskiy I. L. (1983) The thermodynamic parameters of Ag$_2$O(c) and silver(I) hydroxy complexes in aqueous solution at elevated temperatures. *Geochem. Intl.* **20,** 137–149.

Krupp R. E. and Seward T. M. (1987) The Rotokawa geothermal system, New Zealand—An active epithermal gold-depositing environment. *Econ. Geol.* **85,** 1109–1129.

Lieser K. H. (1957) Radiochemische Messung der Löslichkeit von Silberhalogenidea in Wasser und in Natriumhalogeniodlösungen und

die Komplexbildung der Silberhalogenide im Halogenionen. *Z. Anorg. Allgem. Chem.* **292,** 97–113.

McKibben M. A., Andes J. P., and Williams-Jones A. E. (1988) Active ore formation at a brine interface in metamorphosed deltaic lacustrine sediments—The Salton Sea geothermal system, California. *Econ. Geol.* **83,** 511–523.

Mahon W. A. J. and Finlayson J. B. (1972) The chemistry of Broadlands geothermal area, New Zealand. *Am. J. Sci.* **272,** 48–68.

Marshall W. L. and Franck E. U. (1981) Ion product of water substance, 0–1000°C, 1–10,000 bar. New international formulation and its background. *J. Phys. Chem. Ref. Data* **10,** 295–304.

Martell A. E. and Smith R. M. (1989) *Critical Stability Constants.* Plenum, New York.

Martin J.-M. and Whitfield M. (1983) The significance of the river input of chemical elements to the ocean. In *Trace Metals in Seawater* (eds. C. S. Wong, E. Boyle, K. W. Bruland, J. D. Burton, and E. D. Goldberg), pp. 265–296. Plenum, New York.

Melent'yev B. N., Ivanenko V. V., and Pamfilova L. A. (1969) Solubility of some ore-forming sulfides under hydrothermal conditions. *Geochem. Intl.* **7,** 416–460.

Mountain B. M. and Seward T. M. (1999) The hydrosulphide/sulphide complexes of copper(I): Experimental determination of stoichiometry and stability at 22°C and reassessment of high temperature data. *Geochim. Cosmochim. Acta* **63,** 11–29.

Peshchevitsky B. I., Yerenburg A. M., Belevantsev V. I., and Kasakov V. P. (1970) Stability of gold complexes in aqueous solutions. *Izvest. Sib. Otd. Akad. Nauk SSSR, Ser. Khim.* **6,** 126–129.

Ragnarsdóttir K. V., Walther J. V., and Arnórsson S. (1984) Description and interpretation of the composition of fluid and alteration mineralogy in the geothermal system, at Svartsengi, Iceland. *Geochim. Cosmochim. Acta* **48,** 1535–1553.

Renders P. J. and Seward T. M. (1989) The stability of hydrosulphido- and sulphido-complexes of Au(I) and Ag(I) at 25°C. *Geochim. Cosmochim. Acta* **53,** 245–253.

Robie R. A., Hemingway B. S., and Fisher J. R. (1979) Thermodynamic properties of minerals and related substances at 298.15 K and 1 bar (105 pascals) pressures and at higher temperatures. *U.S. Geol. Surv. Bull.* **1452,** 456.

Robinson R. A. and Stokes R. H. (1968) *Electrolyte Solutions.* Butterworths, London.

Schwarzenbach G., Gübeli O., and Züst H. (1958) Thiokomplexe des Silbers und die Löslichkeit von Silbersulfid. *Chimia* **12,** 84–86.

Schwarzenbach G. and Widmer G. (1966) Die Löslichkeit von Metalsulfiden. II. Silbersulfid. *Helv. Chim. Acta* **49,** 111–123.

Seward T. M. (1976) The stability of chloride complexes of silver in hydrothermal solutions up to 350°C. *Geochim. Cosmochim. Acta* **40,** 1329–1341.

Seward T. M. (1989) The hydrothermal chemistry of gold and its implications for ore formation: Boiling and conductive cooling as examples. *Econ. Geol.* **6,** 398–404.

Sugaki A., Scott S. D., Hayashi K., and Kitakaze A. (1987) Ag_2S solubility in sulfide solutions up to 250°C. *Geochem. J.* **21,** 291–305.

Suleimenov O. M. and Krupp R. E. (1994) Solubility of hydrogen sulfide in pure water and in NaCl solutions, from 20 to 320°C and at saturation pressures. *Geochim. Cosmochim. Acta* **58,** 2433–2444.

Suleimenov O. M. and Seward T. M. (1997) A spectrophotometric study of hydrogen sulphide ionisation in aqueous solutions to 350°C. *Geochim. Cosmochim. Acta* **61,** 5187–5198.

Treadwell W. D. and Hepenstick H. (1949) Über die Löslichkeit von Silbersulfid. *Helv. Chim. Acta* **32,** 1872–1879.

Weissberg B. G., Browne P. R. L., and Seward T. M. (1979) Ore metals in active geothermal systems. In *Geochemistry of Hydrothermal Ore Deposits* (ed. H. L. Barnes), pp. 738–780. John Wiley, New York.

Westall J. C. (1982a) *FITEQL: A Computer Program for Determination of Chemical Equilibrium Constants From Experimental Data. Version 1.2.* Department of Chemistry, Oregon State University, Corvallis.

Westall J. C. (1982b) *FITEQL: A Computer Program for Determination of Chemical Equilibrium Constants From Experimental Data. Version 2.0.* Department of Chemistry, Oregon State University, Corvallis.

Wood S. A., Crerar D. A., and Borisck M. P. (1987) Solubility of the assemblage pyrite-pyrrhotite-magnetite-sphalerite-galena-gold-stibine-bismuthinite-argentite-molybdenite in H_2O-NaCl-CO_2 solution from 200 to 350°C. *Econ. Geol.* **82,** 1864–1887.

Xiao Z. F., Gammons C. H., and Williams-Jones A. E. (1998) Experimental study of copper(I) chloride complexing in hydrothermal solutions at 40 to 300°C and saturated water vapor pressure. *Geochim. Cosmochim. Acta* **62,** 2949–2964.

Zotov A. V., Levin K. A., Khodakovskiy I. L., and Kozlov V. K. (1986) Thermodynamic parameters of Ag(I) chloride complexes in aqueous solutions at 273-623 K. *Geochem. Intl.* **23,** 103–116.

Zotov A. V., Levin K. A., Kotova Z. Y., and Volchenkova V. A. (1982) An experimental study of the stability of silver hydroxychloride complexes in hydrothermal solutions. *Geochem. Intl.* **19,** 151–164.

Appendix A.   Analytical results

No.	p/bar	m S mol kg^{-1}	m NaOH mol kg^{-1}	m Ag mol kg^{-1}
		$t = 25$°C		
1	1	0.061	0.000	6.23E-07
2	1	0.048	0.000	4.90E-07
3	1	0.086	0.000	8.30E-07
4	1	0.101	0.008	1.12E-06
5	1	0.059	0.004	7.20E-07
6	1	0.110	0.006	1.16E-06
7	1	0.115	0.008	1.15E-06
8	1	0.127	0.008	1.09E-06
9	1	0.053	0.000	4.97E-07
10	1	0.007	0.000	1.85E-07
11	1	0.131	0.053	2.70E-06
12	1	0.043	0.040	3.75E-07
13	1	0.131	0.080	3.09E-06
14	1	0.101	0.113	5.52E-07
15	1	0.039	0.108	1.02E-07
16	1	0.122	0.112	2.03E-06
17	1	0.176	0.210	1.94E-06
		$t = 50$°C		
18	1	0.100	0.000	6.56E-07
19	1	0.129	0.030	2.62E-06
20	1	0.015	0.000	2.40E-07
21	1	0.041	0.033	9.12E-07
22	1	0.112	0.010	8.91E-07
23	1	0.087	0.103	5.62E-07
24	1	0.121	0.093	3.87E-06
25	1	0.062	0.047	1.23E-06
26	1	0.162	0.210	2.86E-06
		$t = 100$°C		
27	10	0.018	0.000	2.75E-07
28	10	0.021	0.000	2.98E-07
29	10	0.079	0.015	2.25E-06
30	10	0.066	0.039	3.30E-06
31	10	0.079	0.015	2.25E-06
32	10	0.048	0.095	1.75E-07
33	10	0.120	0.041	5.87E-06
34	10	0.060	0.085	2.79E-07

$t = 100°C$

35	10	0.097	0.098	1.14E-06
36	10	0.110	0.109	2.48E-06
37	10	0.107	0.061	6.54E-06
38	500	0.018	0.000	3.10E-07
39	500	0.021	0.015	5.60E-07
40	500	0.079	0.015	1.48E-06
41	500	0.066	0.039	3.18E-06
42	500	0.047	0.307	2.40E-07

$t = 150°C$

43	20	0.103	0.000	8.10E-07
44	20	0.018	0.000	3.10E-07
45	20	0.015	0.015	2.70E-07
46	20	0.086	0.015	4.57E-06
47	20	0.121	0.039	9.70E-06
48	20	0.028	0.095	1.16E-07
49	20	0.062	0.047	6.11E-06
50	20	0.162	0.210	2.45E-06
51	500	1.026E-01	0.000	5.70E-07
52	500	1.780E-02	0.000	1.50E-07
53	500	1.509E-02	0.015	2.30E-07
54	500	8.572E-02	0.015	3.79E-06
55	500	1.209E-01	0.039	8.13E-06
56	500	4.200E-02	0.297	1.80E-07

$t = 200°C$

57	40	0.105	0.000	8.00E-07
58	40	0.015	0.000	2.80E-07
59	40	0.016	0.015	1.22E-06
60	40	0.086	0.015	8.14E-06
61	40	0.121	0.039	2.35E-05
62	40	0.105	0.000	7.50E-07
63	40	0.086	0.015	8.04E-06
64	40	0.068	0.095	1.60E-06
65	40	0.052	0.250	7.70E-07
66	500	0.015	0.000	4.20E-07
67	500	0.016	0.015	1.19E-06
68	500	0.086	0.015	8.07E-06
69	500	0.121	0.039	2.19E-05
70	500	0.051	0.309	6.30E-07

$t = 250°C$

71	60	0.098	0.000	6.39E-07
72	60	0.015	0.000	2.90E-07
73	60	0.016	0.015	2.72E-06
74	60	0.091	0.015	1.24E-05
75	60	0.121	0.039	3.35E-05
76	60	0.028	0.095	1.05E-06

$t = 250°C$

77	60	0.030	0.200	4.99E-07
78	60	0.103	0.203	5.42E-06
79	60	0.026	0.317	3.23E-07
80	500	0.098	0.000	6.39E-07
81	500	0.015	0.000	2.90E-07
82	500	0.016	0.015	2.11E-06
83	500	0.121	0.039	2.68E-05
84	500	0.034	0.407	3.31E-07

$t = 300°C$

85	110	0.098	0.000	6.57E-07
86	110	0.014	0.000	1.98E-07
87	110	0.016	0.015	4.10E-06
88	110	0.091	0.015	2.31E-05
89	110	0.121	0.039	5.21E-05
90	110	0.091	0.015	2.53E-05
91	110	0.068	0.095	8.30E-06
92	110	0.107	0.052	6.12E-05
93	110	0.053	0.027	1.87E-05
94	110	0.093	0.053	5.02E-05
95	500	1.559E-02	1.500E-02	2.87E-06
96	500	9.063E-02	1.500E-02	2.52E-05
97	500	1.120E-01	4.100E-02	5.62E-05
98	500	9.700E-02	0.000E+00	6.80E-07

$t = 350°C$

99	200	0.014	0.000	1.69E-07
100	200	0.016	0.015	4.53E-06
101	200	0.091	0.015	2.86E-05
102	200	0.121	0.039	6.07E-05
103	200	0.028	0.095	2.97E-06
104	200	0.108	0.000	5.25E-07
105	200	0.118	0.042	5.70E-05
106	200	0.095	0.057	6.81E-05
107	500	0.091	0.015	2.24E-05
108	500	0.121	0.039	8.52E-05
109	500	0.052	0.000	4.33E-07
110	500	0.097	0.000	7.90E-07

$t = 400°C$

111	500	0.016	0.015	7.52E-06
112	500	0.091	0.015	4.76E-05
113	500	0.121	0.039	1.30E-04
114	500	0.107	0.052	1.17E-04
115	500	0.053	0.027	3.75E-05
116	500	0.093	0.053	8.85E-05
117	500	0.025	0.000	2.00E-07
118	500	0.053	0.000	3.10E-07

Appendix B. Logarithms of the equilibrium constants used for aqueous speciation calculation

Reaction	p/bar	t/°C									Ref.
		25	50	100	150	200	250	300	350	400	
$H_2O = H^+ + OH^-$	swvp	−14.00	−13.28	−12.27	−11.64	−11.29	−11.19	−11.41	−12.30		a
	500			−12.10	−11.45	−11.05	−10.85	−10.86	−11.14	−11.88	a
$NaOH(aq) = Na^+ + OH^-$	swvp	0.72	0.48	0.07	−0.27	−0.59	−0.92	−1.29	−1.84		b
	500			0.07	−0.26	−0.56	−0.86	−1.17	−1.54	−2.05	b
$NaHS(aq) = Na^+ + HS^-$	swvp	1.18	1.00	0.68	0.38	0.07	−0.29	−0.73	−1.46		c
	500			0.72	0.43	0.14	−0.16	−0.51	−0.95	−1.59	c
$H_2S(aq) = H^+ + HS^-$	swvp	−6.99	−6.68	−6.49	−6.49	−6.73	−7.19	−7.89	−8.89		d
	500			−6.32	−6.36	−6.55	−6.88	−7.32	−7.92	−8.92	e
$0.5Ag_2S(s) + H^+ = Ag^+ + 0.5H_2S(aq)$	swvp	−14.5	−13.2	−10.9	−9.1	−7.7	−6.7	−5.8	−5.1		f
$0.5Ag_2S(s) + H_2O = AgOH(aq) + 0.5H_2S(aq)$	swvp	−26.5	−24.6	−21.5	−19.0	−17.1	−15.7	−14.5	−13.5		f
$0.5Ag_2S(s) + 2H_2O = Ag(OH)_2^-(aq) + 0.5H_2S(aq) + H^+$	swvp	−38.3	−36.0	−32.1	−29.1	−26.8	−25.0	−23.5	−22.3		f

swvp = saturated water vapour pressure.
[a] Marshall and Franck (1981).
[b] Ho and Palmer (1996).
[c] Taken to be the same as for the reaction $NaCl(aq) = Na^+ + Cl^-$ using values reported by Ho et al. (1994).
[d] Suleimenov and Seward (1997).
[e] Corrected for pressure using ΔV_r given by Ellis and McFadden (1972).
[f] See text.